Chapter 3

Thermo-Oxidative Decomposition and Residue Formation in Esters: Implications for 55Al-43.4Zn-1.6Si Metallic Coating Quality

Preface

This Chapter examines the thermal decomposition of a variety of methyl esters (3.1) and naturally occurring triglycerides and commercial cold rolling oil base esters (3.2) under an oxygen atmosphere. Thermogravimetric Analysis (TGA) and Pressure Differential Scanning Calorimetry (PDSC) test conditions are used to simulate the continuous annealing process, whereby rolling oil is removed from the surface of cold rolled steel strip. Relationships between ester structure and the amount/chemical nature of residue present at the average maximum continuous annealing temperature (~ 500 ^{o}C) are assessed. The impact of persistent triglyceride and base ester residues on 55Al-43.4Zn-1.6Si coating quality is determined by performing industrial-scale hot dipping trials. The results show that in the presence of oxygen, highly unsaturated esters decompose to leave significant amounts of thermally-stable residue. This residue consists of 'soap-like' complexes and non-volatile oxygenated products and it gives rise to uncoated defects in 55Al-43.4Zn-1.6Si.

3.1 Effect of Alkyl Chain Unsaturation on Thermo-Oxidative Decomposition and Residue Formation in Methyl Esters

3.1.1 Introduction

Esters form the basis of a wide variety of products in the food, coatings, automotive and metal processing industries. Consequently, the mechanism of ester decomposition in the presence of oxygen has a significant impact on our everyday lives. Controlling the oxidative reactions of naturally occurring esters (fats and oils) is critical within the food

industry.[1-3] The stability of edible fats and oils towards oxidation affects both shelf life and processability,[4, 5] whilst the products of oxidation reactions impart a repugnant flavour and odour to food.[1, 2] Crosslinking reactions undergone by unsaturated esters during oxidation are essential to the formation of durable paint and varnish films within the coatings industry[1, 6] but detrimental in the automotive and metal industries; these reactions have been associated with the formation of deposits that give rise to wear and failure in mechanical systems[7-13] or downstream coating problems in sheet metal processing.[14, 15] Given the industrial significance of ester oxidation, particularly in relation to the use of esters as lubricants in high temperature applications where preventing the formation of thermally stable residues is critical, a fundamental understanding of the oxidation process and its dependency on conditions such as temperature and ester chemical structure is of utmost importance.

The oxidative stability of fatty acid methyl esters has been the focus of extensive research as a result of the wide use of these esters within the food and drug industries.[16] Fatty acid methyl esters are typified by the structure given in scheme 3.1 below.

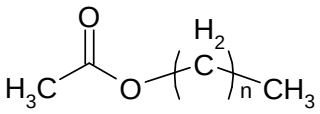

Scheme 3.1 Representation of a typical fatty acid methyl ester structure, where n = 3-21.

Methyl esters are often given the notation C*x*:*y* (such as C18:0 for methyl stearate), where *x* is the number of carbon atoms in the ester alkyl chain (typically between 4 and 22) and *y* is the number of carbon-carbon double bonds (between 0 and 5).[1] The mechanisms involved in the low temperature auto-oxidation of methyl oleate (C18:1), methyl linoleate (C18:2) and methyl linolenate (C18:3) have been extensively characterised using traditional chemical analysis techniques such as GCMS, FTIR and HPLC.[17, 18] As described in detail in section 1.2.3.1 in Chapter 1, the auto-oxidation process of an unsaturated ester can be summarised as:[1-3, 5, 6, 18, 19]

- reaction initiation (usually catalysed by heat, light or transition metals);
- hydroperoxide (ROOH) formation involving the uptake of molecular oxygen and hydrogen atom abstraction from the hydrocarbon substrate;
- hydroperoxide decomposition to form a range of reactive radical species;
- polymerisation via radical addition to carbon-carbon double bonds (C=C), and
- radical side reactions to produce secondary oxidation products such as aldehydes, ketones, carboxylic acids and alcohols.

Despite this detailed knowledge, the oxidation process of fatty acid methyl esters has not been studied under controlled heating conditions. Furthermore, very little is reported on the subsequent thermal decomposition reactions undergone by methyl ester oxidation products, or the chemical nature of the thermally stable residues which cause problems in surface coating applications. Whilst TGA and PDSC have been used to study the thermal decomposition of a variety of synthetic,[10, 11] semi-synthetic[10] and naturally occurring (triglyceride)[2-5, 19, 20] tri-esters under oxidising conditions, the use of such techniques to study long chain fatty acids/methyl esters has only been reported at low (< 200 ^{o}C) temperatures[21] and under nitrogen.[16]

In this study, the effect of alkyl chain unsaturation levels on the thermo-oxidative decomposition of a model system consisting of methyl stearate (C18:0), methyl oleate (C18:1), methyl linoleate (C18:2) and methyl linolenate (C18:3) esters has been investigated using TGA, PDSC and Attenuated Total Reflectance FTIR (ATR) techniques. The residue formation processes undergone by each methyl ester are assessed independently, avoiding the complexities associated with higher esters.[9]

3.1.2 Experimental

3.1.2.1 Sample Preparation

3.1.2.1.1 Materials

The methyl stearate, methyl oleate, methyl linoleate and methyl linolenate samples studied in this section were obtained from Nu-Chek Prep Inc. (Elysian, Minnesota) and

were of > 99 % purity. All samples were kept in the dark and under nitrogen to minimise oxidation during storage. The oxygen gas and TGA/PDSC consumables used are described in Chapter 2 (sections 2.2.6 and 2.2.7, respectively).

3.1.2.1.2 Sample Preparation for ATR

Methyl ester samples were prepared for mid-infrared ATR analysis according to the procedure described in section 2.3.2 in Chapter 2. Additional samples were created at 215 ^{o}C, 220 ^{o}C and 240 ^{o}C to enable a more accurate characterisation of the methyl ester decomposition process.

3.1.2.2 Characterisation of Thermal Decomposition Behaviour

3.1.2.2.1 TGA

TGA analysis of the methyl esters was carried out under oxygen according to the conditions and procedure described in section 2.4.1 in Chapter 2.

3.1.2.2.2 PDSC

PDSC analysis of the methyl esters was carried out according to the conditions and procedure described in section 2.4.2 in Chapter 2.

3.1.2.2.3 ATR

Spectra of the ester samples outlined above were collected according to the mid-infrared analysis method detailed in section 2.4.3.1 in Chapter 2.

3.1.3 Results and Discussion

3.1.3.1 Thermo-Oxidative Decomposition Profile by TGA

TGA analysis of four methyl esters of varying unsaturation levels was performed. Figure 3.1 shows a typical TGA thermogram for the decomposition of methyl stearate under

oxygen. Both the mass loss with respect to temperature (TG) and the first derivative of mass loss with respect to temperature (DTG) curves are shown.

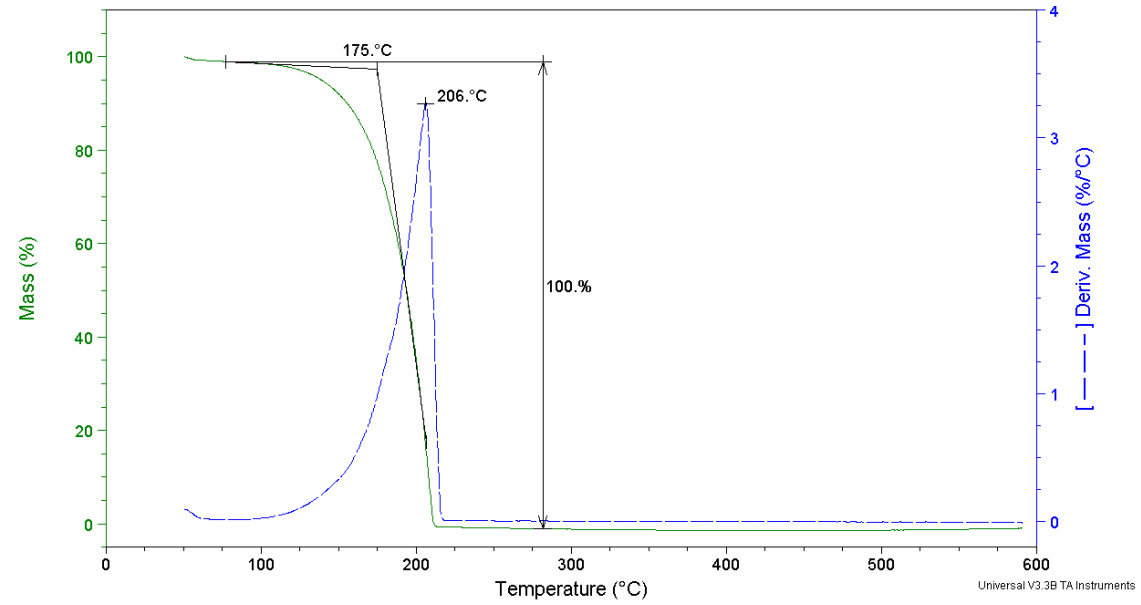

Figure 3.1 Methyl stearate thermo-oxidative decomposition profile by TGA.

The methyl stearate thermo-oxidative mass loss process proceeds via a single step and essentially the entire sample mass is lost by 220 ^{o}C. The onset temperature of mass loss (onset point, T_{onset}) occurs at an average value of 176 ^{o}C and the maximum rate of mass loss temperature (peak temperature, T_{max}) is ~ 206 ^{o}C. The rate of mass loss (DTG) curve is not perfectly Gaussian in shape; the initial stages of sample mass loss proceed more slowly than the latter stages such that over 70 % mass loss occurs before the peak temperature is reached. This change in rate of mass loss after the peak temperature is indicative of a change in the mechanism by which volatiles are being evolved. Similar findings were reported by Gamlin et al.[10] for the decomposition of engine base oils, whereby after 60 % mass loss the order of the decomposition reaction was found to change.

Figure 3.2 compares the DTG results for the four methyl esters under oxygen and a summary of the onset points (T_{onset}), peak and shoulder temperatures (T_{max}) and the relevant mass losses is presented in table 3.1.

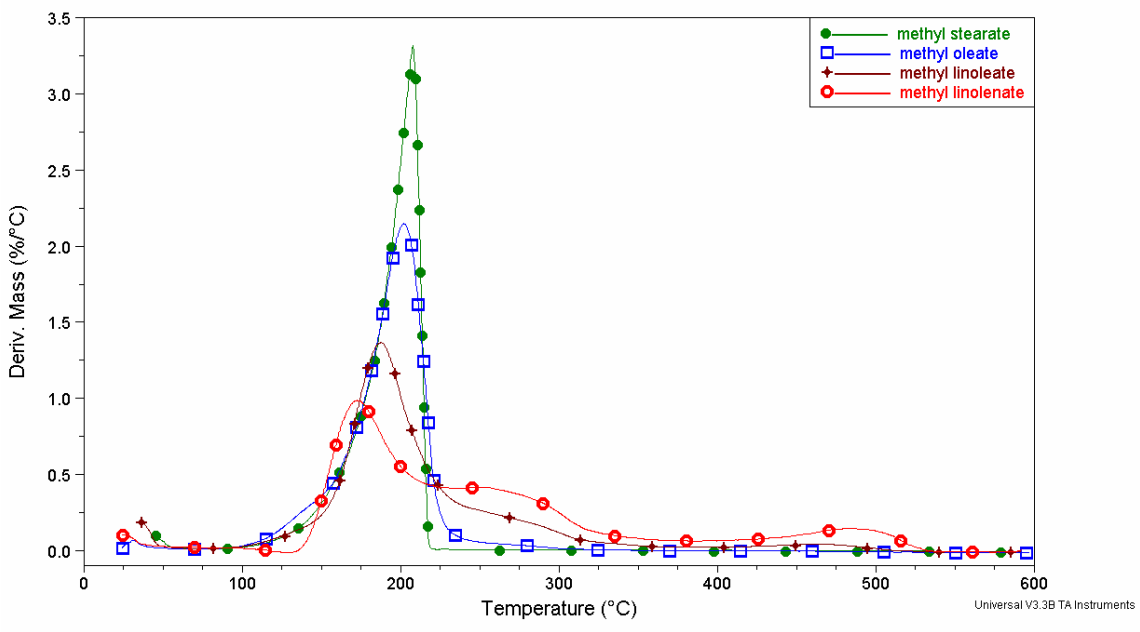

Figure 3.2 Overlay of the TGA thermo-oxidative decomposition profiles (DTG curves) of methyl stearate, methyl oleate, methyl linoleate and methyl linolenate.

In contrast to methyl stearate, the decomposition processes for methyl oleate, methyl linoleate and methyl linolenate involve multiple overlapping mass loss events. Despite this, the DTG curves in figure 3.2 show that volatile products are being evolved over the entire temperature range of decomposition for each of the esters and that no significant amounts of residue (> 0.5 %) are present at 500 ^{o}C. The results in table 3.1 show that increasing the level of oil unsaturation shifts the onset point for oil mass loss to lower temperature. This observation is in accordance with the findings of Sathivel et al.,[3] who observed that the onset temperature of mass loss under nitrogen followed the progression C18:0 > C18:1 > C18:2. This trend was attributed to a decrease in the heat resistance of C18 fatty acids with increasing levels of unsaturation. Under an oxidising

atmosphere it can be expected that the decrease in onset temperature with increasing oil unsaturation is due to a combination of the decreased heat resistance of unsaturated oils together with the greater susceptibility of these oils to oxidation.

Table 3.1 Summary of TGA thermo-oxidative decomposition data for the four methyl esters. Errors are less than ± 5 %.

Ester	T_{onset} (°C)	O_2 Uptake (%)	T_{max} Event 1 (°C)	Mass Loss Event 1 (%)	T_{max} Event 2 (°C)	Mass Loss Event 2 (%)	T_{max} Event 3 2 (°C)	Mass Loss Event 3 (%)
Methyl stearate (C18:0)	176	-	207	100	-	-	-	-
Methyl oleate (C18:1)	167	-	202	96.0	259	3.97	-	-
Methyl linoleate (C18:2)	159	-	186	76.0	260	17.8	463	3.31
Methyl linolenate (C18:3)	154	0.2	172	54.2	254	34.2	485	12.4

In contrast to observations made in the literature,[2, 3, 5] methyl linolenate was the only unsaturated methyl ester sample for which the thermo-oxidative decomposition process was initiated by an oxygen uptake mechanism; no mass increase was observed for the methyl oleate or methyl linoleate samples.

These differences can be reconciled by considering the experimental conditions employed during TGA analysis and the relative reactivities of the unsaturated methyl esters towards oxidation initiation (described by schemes 1.9-1.10 in Chapter 1).[6] Given the ramped heating conditions employed and the limited exposure of the ester samples to

the metal catalyst (the aluminium pan surface), the oxidation initiation step is likely to be slow, limiting the radical species available for reaction with molecular oxygen.[1, 22] In addition, highly unsaturated esters, particularly those containing conjugated double bond systems, are considerably more susceptible to hydrogen abstraction than their more saturated counterparts.[6] Therefore, whilst methyl linolenate undergoes a discernable mass increase of 0.2 % associated with oxygen uptake, the oxygen uptake of methyl linoleate and oleate is shifted to increasingly higher temperatures so that it is masked by simultaneous mass loss processes such as sample evaporation.

The decomposition of methyl oleate involves two mass loss events; event 1, a peak in the DTG curve at 202 ^{o}C (96 % mass loss) is followed by a high temperature mass loss shoulder (event 2) at approximately 259 ^{o}C (4.0 % mass loss). There is possibly also a low temperature shoulder on event 1, however it is not easily definable and was not observed in all three methyl oleate TGA runs. The methyl linoleate decomposition pattern is even more complex, consisting of a peak corresponding to event 1 at 186 ^{o}C (76.0 % mass loss), event 2 at 260 ^{o}C (17.8 % mass loss) and event 3 at 463 ^{o}C (3.3 % mass loss). Analogous results are obtained for methyl linolenate (event 1 at 172 ^{o}C, 54.2 % mass loss; event 2 at 254 ^{o}C, 34.2 % mass loss; event 3 at 485 ^{o}C, 12.4 % mass loss).

These findings show that the presence and level of unsaturation within the methyl ester alkyl chain has a dramatic effect on the thermo-oxidative decomposition process. The temperature at which decomposition is complete is highly dependent on the presence of C=C bonds; whilst methyl stearate was fully decomposed by ~ 220 ^{o}C, the decomposition of methyl oleate, methyl linoleate and methyl linolenate was not complete until ~ 320 ^{o}C, 500 ^{o}C and 525 ^{o}C respectively. In addition, significantly greater amounts of thermally stable residue were formed for the methyl oleate, methyl linoleate and methyl linolenate samples.

These observations can be rationalised by considering the chemical processes via which each of the methyl esters decomposes. The mass loss processes undergone by methyl stearate could potentially include evaporation, ester decarboxylation, thermal cracking and combustion, as outlined by schemes 1.17-1.20 in Chapter 1.[23] It is therefore likely

that evaporation dominates the early stages of methyl stearate mass loss and that the latter stages are due to thermo-oxidative decomposition.[24]

Methyl oleate could undergo the same reactions and processes as methyl stearate, however the presence of a single C=C bond provides an opportunity for thermal and/or metal-catalysed oxidation to occur.[1, 17, 18] The processes involved during oxidation, described in detail by schemes 1.9-1.16 in Chapter 1, can be generalised as including reaction initiation, the formation of free radical species via oxygen uptake and hydroperoxide decomposition, the formation of volatile products such as aldehydes, acids and ketones via the side reactions of radicals, and the formation of non-volatile, high molecular weight oxidation products via radical addition (propagation) to C=C bonds.[1, 6, 18, 19] Importantly, the polymerised products formed by radical addition reactions in methyl oleate do not allow for the formation of crosslinked network-type polymers; instead, the polymers formed are likely to be branched in nature (scheme 3.2).

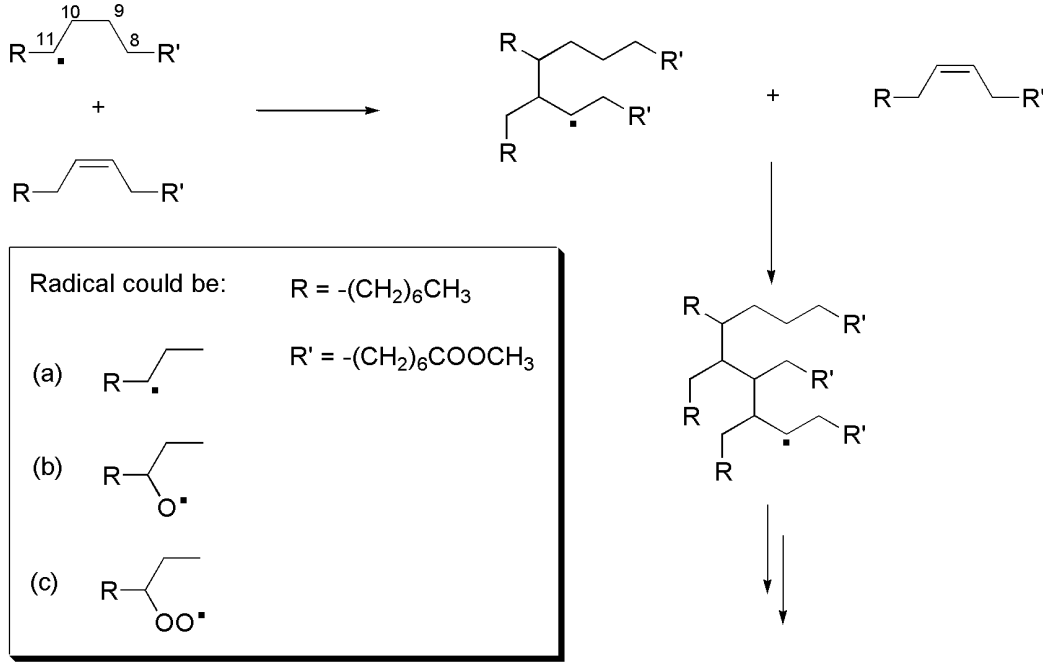

Scheme 3.2 Schematic representation of the addition (propagation) reactions undergone by methyl oleate to form a branched polymer.

In light of these considerations, mass loss event 1 observed for methyl oleate represents a combination of sample evaporation, radical formation and the evolution of volatiles produced via the side reactions of radical species. Mass loss event 2 results from the volatilisation and thermal decomposition of high molecular weight material formed by radical addition to the C=C bond in the oleate alkyl chain and recombination (termination) reactions (note that radical addition and recombination reactions do not result in mass loss, however they are likely to compete with side reactions during the first mass loss event). The reactions involved in thermal decomposition are similar to those described for methyl stearate above.

The reactions of methyl linoleate and methyl linolenate are analogous to those of methyl oleate, however the presence of multiple C=C bonds means that inter- and intra-molecular crosslinking can occur between ester alkyl chains to form a network polymer (scheme 3.3).[6, 18]

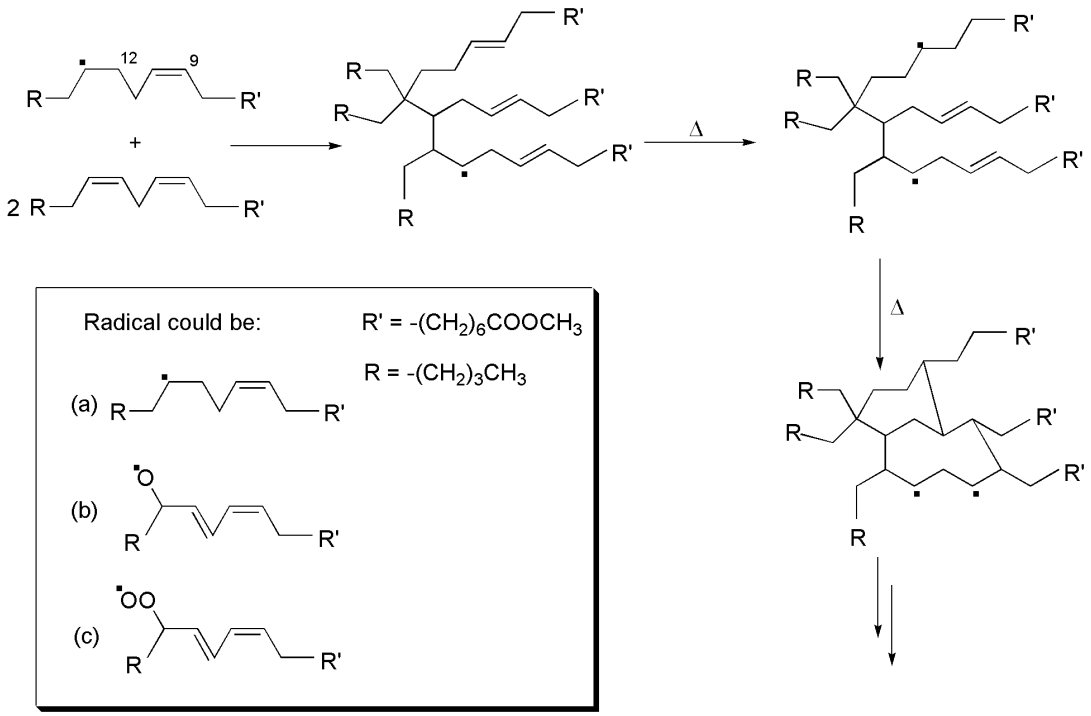

Scheme 3.3 Schematic representation of the crosslinking reactions undergone by methyl linoleate to form a network polymer.

Therefore, the additional mass loss event (event 3) observed for methyl linoleate and methyl linolenate results from the decomposition of networked deposits as a consequence of the higher thermal stability of this material.[25] At this stage it should be noted that the methyl linoleate and linolenate decomposition processes are most representative of the thermo-oxidative reactions of triglycerides and rolling oil base esters as these esters can potentially form network-like structures by intra- and inter-molecular crosslinking between unsaturated fatty acid chains.

3.1.3.2 Thermo-Oxidative Decomposition Profile by PDSC

Figure 3.3 shows an overlay of the heat flow vs. temperature plots obtained by constant-volume PDSC analysis of the four methyl esters. The onset points (T_{onset}), peak and shoulder temperatures (T_{max}) and enthalpies are given in table 3.2.

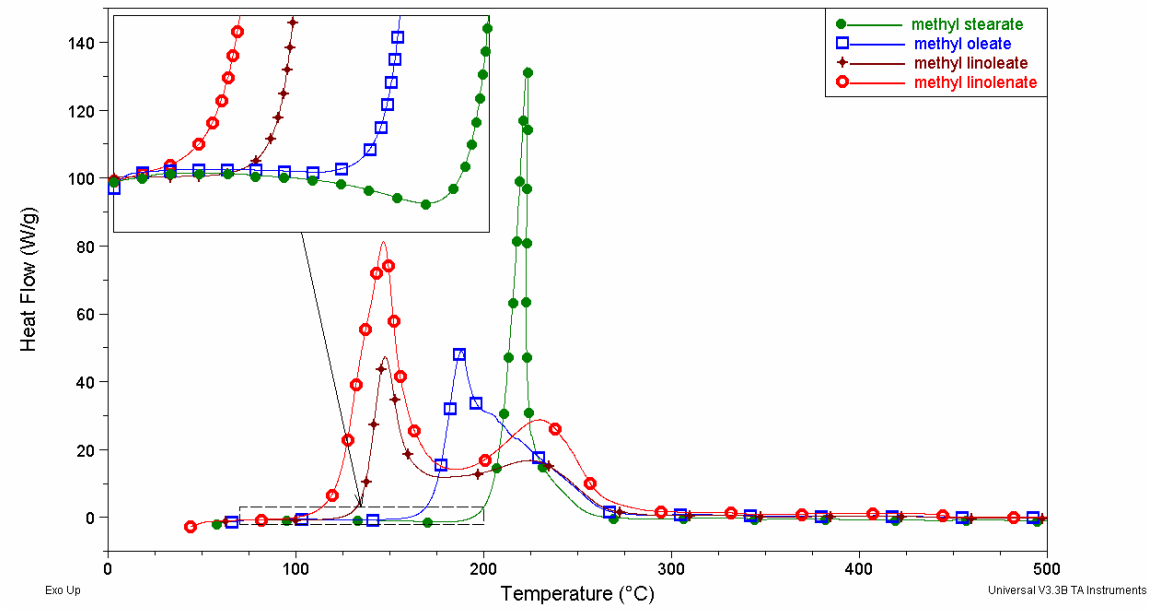

Figure 3.3 Overlay of the PDSC thermograms of methyl stearate, methyl oleate, methyl linoleate and methyl linolenate. The inset highlights the evaporation endotherm observed for methyl stearate.

The thermo-oxidative decomposition of methyl stearate is preceded by an endotherm at ~ 179 ^{o}C (see figure 3.3 inset) that is due to a small amount of sample evaporation despite the high pressure employed during testing.[19] This endotherm is followed immediately by a sharp exotherm at 222 ^{o}C that contributes to 97.0 % of the total heat flow and evidences ignition of the ester sample.[10] Finally, a broad, tail-like region accounting for only 3.0 % of the total heat flow occurs at ~ 314 ^{o}C. This region comprises of multiple overlapping exothermic and endothermic transitions representing the thermal cracking and combustion of residual carbonaceous material.[7, 8, 23] Processes such as reaction initiation and the evaporation of volatiles give rise to endotherms, whilst combustion and the propagation of thermal cracking reactions correspond to exotherms.[7] The number and characteristics (such as peak temperature and enthalpy) of these endothermic and exothermic events vary considerably between runs. This is due to variations in the composition of the partially decomposed sample arising from small differences in the initial sample mass and geometry as well as the extent of ignition reaction at 222 ^{o}C.[26] The evolution of volatile products during the thermo-oxidative decomposition of methyl stearate therefore involves numerous processes and reactions that are highly interdependent and occur up to high temperatures (> 500 ^{o}C) despite the TGA results showing that the majority of the sample has been volatilised at 220 ^{o}C.

Introducing a centre of unsaturation into the ester alkyl chain, as per the case for methyl oleate, generates notable differences in the PDSC heat flow profile. The onset temperature for thermo-oxidative decomposition of methyl oleate is ~ 30 ^{o}C lower than that observed for methyl stearate and no sample evaporation is evident. Like methyl stearate, methyl oleate decomposes via two dominant exothermic events represented by a broad peak at ~ 188 ^{o}C (96.6 % of the total heat flow) and a tail-like peak at ~ 319 ^{o}C (3.4 % of the total heat flow). The broad exothermic event at 188 ^{o}C contains at least three overlapping exotherms that evidence the generation of free radicals, followed by the reactions of these radicals to form either volatile secondary oxidation products or high molecular weight deposits.[17, 18]

Table 3.2 Summary of PDSC data obtained for the four methyl esters. Errors are less than ± 10 %.

Ester	T_{max} Endotherm 1 (^oC)	ΔH Endotherm 1 ($J g^{-1}$)	T_{onset} (^oC)	Primary Region Room Temperature-300 ^oC				Secondary Region > 300 ^oC	
				T_{max} Exotherm 1 (^oC)	ΔH Exotherm 1 ($J g^{-1}$)	T_{max} Exotherm 2 (^oC)	ΔH Exotherm 2 ($J g^{-1}$)	T_{max} tail-like region (^oC)	ΔH tail-like region ($J g^{-1}$)
Methyl stearate (C18:0)	179	137	207	222	9020	-	-	314	282
Methyl oleate (C18:1)	-	-	174	188*	12000	-	-	319	419
Methyl linoleate (C18:2)	-	-	136	148	6080	226	7030	310	511
Methyl linolenate (C18:3)	-	-	121	147	14600	230	10500	328	1050

* Exotherm 1 for methyl oleate comprises of approximately three overlapping exotherms at ~ 188 ^{o}C, 202 ^{o}C and 221 ^{o}C.

The trend towards lower onset temperature and increased complexity of thermo-oxidative decomposition with increasing ester unsaturation is continued for methyl linoleate and methyl linolenate. These ester show decomposition onset temperatures of only 136 ^{o}C (methyl linoleate) and 121 ^{o}C (methyl linolenate) and both decompose via three, as opposed to two, exothermic events. The first occurs at ~ 148 ^{o}C, accounts for 44.7 % (methyl linoleate) and 55.8 % (methyl linolenate) of the total heat flow and represents the formation of free radical species. The third net exothermic event is the 'tail like' region common to all four esters, which accounts for 3.7 % (methyl linoleate) and 4.0 % (methyl linolenate) of the total heat flow and contains multiple overlapping events that involve the decomposition of residual carbonaceous deposits.[7, 8] The second exotherm with a peak maximum of 226 ^{o}C accounts for 51.6 % (methyl linoleate) and 40.2 % (methyl linolenate) of the total heat flow. Interestingly, the temperature at which this exotherm occurs is similar to that of the third overlapping exotherm in the methyl oleate thermogram (~ 220 ^{o}C). The ~ 202 ^{o}C exotherm in the PDSC results for methyl oleate has no counterpart in the methyl linoleate and methyl linolenate results, either because the reactions giving rise to this event do not occur, or because they are so insignificant as to be obscured by the surrounding exotherms. This observation can be rationalised by considering the relative reactivity of conjugated as opposed to non-conjugated systems. The C=C bonds present in conjugated systems are considerably more susceptible to addition by radical species than non-conjugated C=C bonds.[6, 18] It has been suggested that the peroxide radicals formed by oxygen uptake may add directly to conjugated double bonds without first forming hydroperoxides by hydrogen atom abstraction.[6] Consequently, during the oxidation of methyl linoleate and methyl linolenate, the consumption of C=C bonds will occur more rapidly at lower temperatures than radical decomposition or recombination reactions. Given this, it is likely that the exotherm at 202 ^{o}C observed only for methyl oleate (and obscured in the methyl linoleate and methyl linolenate results) represents the addition of radicals species to C=C bonds in the ester alkyl chain and that the recombination and side reactions of remaining radical species dominate the exotherm present for all three unsaturated esters at 220 ^{o}C.

A comparison between the TGA and PDSC onset points for the four esters shows that whilst the onset point by TGA decreases marginally with increasing oil unsaturation, the onset point obtained by PDSC decreases quite dramatically (figure 3.4).

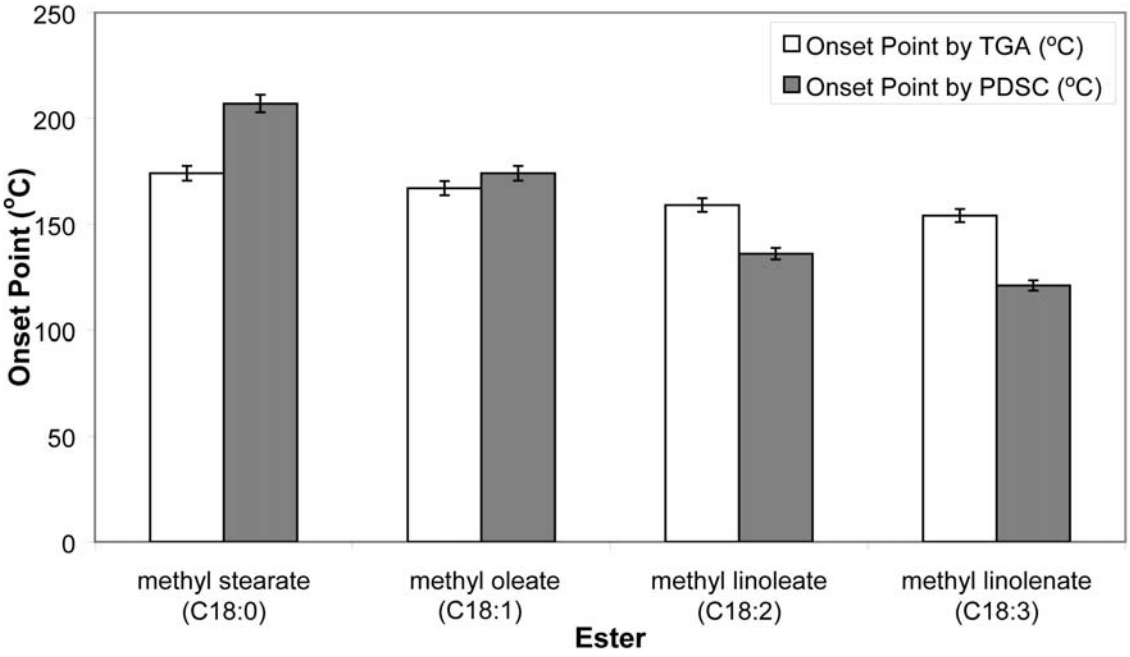

Figure 3.4 Comparison between mass loss (TGA) and oxidation (PDSC) onset temperatures for methyl stearate, methyl oleate, methyl linoleate and methyl linolenate. The error bars represent ± 2 % error.

For methyl stearate the onset point by PDSC is significantly greater than by TGA, however for methyl oleate the two onset temperatures are comparatively similar and for methyl linoleate, the TGA onset temperature exceeds the onset temperature measured by PDSC. In fact, for the methyl linoleate sample, ~ 4260 J g^{-1} of heat flow occurs before the TGA onset point of 159 ^{o}C. These observations suggest that highly unsaturated esters undergo exothermic reactions at low temperatures (such as crosslinking to form high molecular weight polymeric deposits) that do not result in the production of volatile material.

3.1.3.3 Evaluation of Residue Levels by the % B/A Ratio Technique

The tendency for each of the esters to form thermally stable deposits can be measured by calculating the % B/A ratio according to equation 3.1 below: [7, 8]

$$\% \text{ B/A Ratio} = \frac{B}{A} \times 100 \qquad \text{Equation 3.1}$$

where:

- B (secondary decomposition region) = the percentage of sample mass lost between 240 ^{o}C and 500 ^{o}C (TGA) or the total heat flow associated with events occurring between 300 ^{o}C and 500 ^{o}C (PDSC), and
- A (primary decomposition region) = the percentage of sample mass lost between room temperature and 240 ^{o}C (TGA) or the total heat flow associated with events occurring between room temperature and 300 ^{o}C (PDSC).

The temperature regions over which 'A' and 'B' are calculated are defined such that processes predominantly leading to the creation of thermally stable deposits (oxidation, crosslinking) are included within 'A' and processes which destroy deposits (combustion and thermal cracking of high molecular weight material) are included within 'B'. It should be noted that sample evaporation is also included within 'A' despite the fact that it does not lead to the formation of deposits. Figure 3.5 shows a plot of the % B/A ratio, calculated from PDSC and TGA thermograms using equation 3.1, against the number of C=C bonds in the ester alkyl chain.

The % B/A ratio determined by TGA increases in an exponential fashion with respect to increasing alkyl chain unsaturation. This observation is in good agreement with the thermo-oxidative decomposition mechanisms proposed above; polyunsaturated methyl esters are capable of forming crosslinked deposits that persist until high temperatures, giving rise to a significant mass loss over the 'B' region. The corresponding increase in the % B/A ratio by PDSC is only small; the enthalpies associated with events in both the primary and secondary regions increase with increasing unsaturation. Consequently,

alkyl chain unsaturation levels have a greater effect on the amount of thermally stable material that is removed at higher temperatures as opposed to the energy required to remove this material.

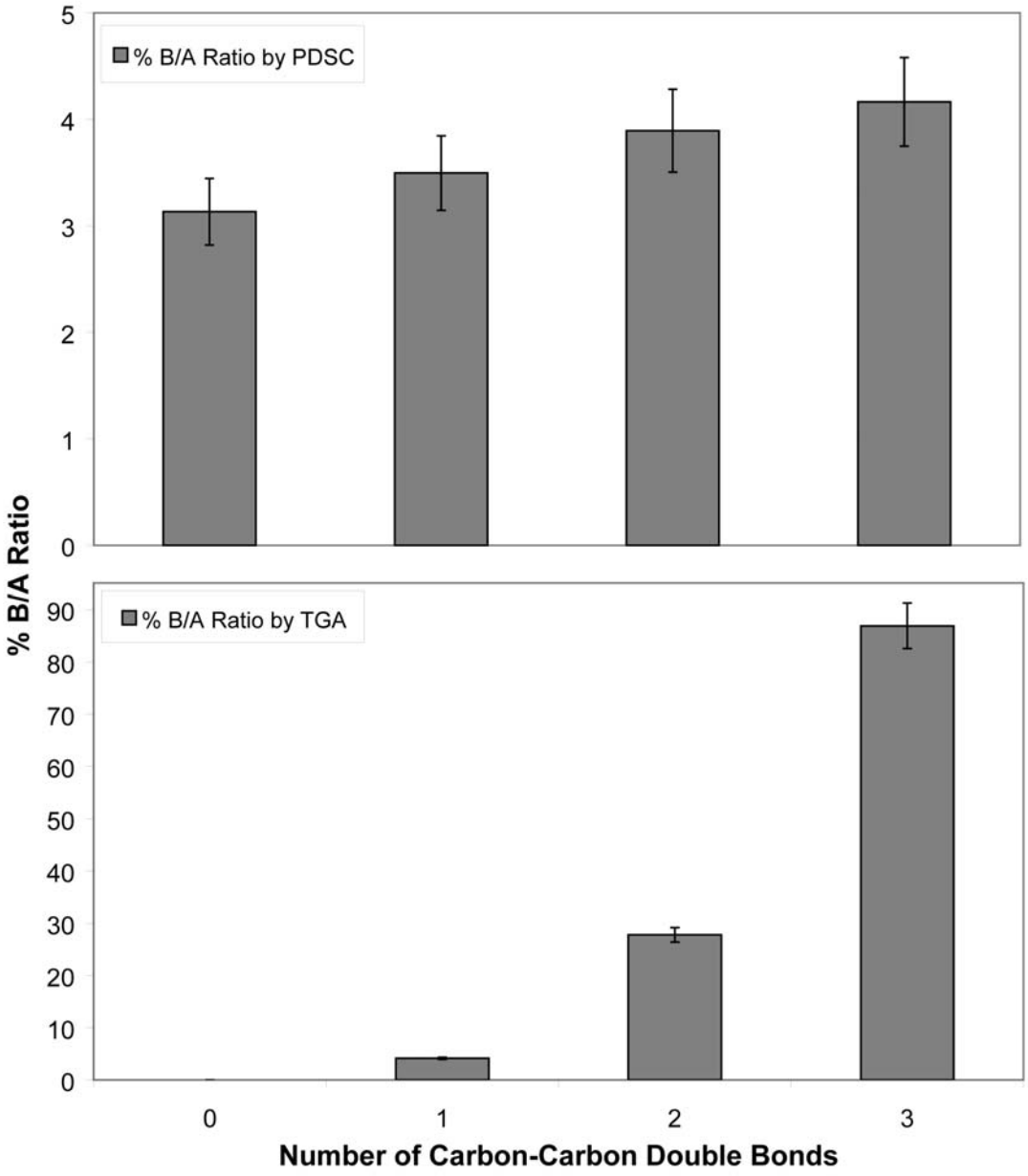

Figure 3.5 % B/A ratio vs. the number of C=C bonds in the ester alkyl chain. The error bars represent ± 5 % error (TGA) and ± 10 % error (PDSC).

3.1.3.4 ATR Characterisation of Thermo-Oxidative Decomposition Reactions

The thermo-oxidative decomposition chemistry of the methyl esters was studied by ATR. The room temperature spectra collected for the four methyl ester samples are similar, therefore a representative ATR spectrum for methyl linoleate at room temperature is given in figure 3.6. The peak assignments for the spectra acquired for each of the methyl esters are detailed in table 3.3.

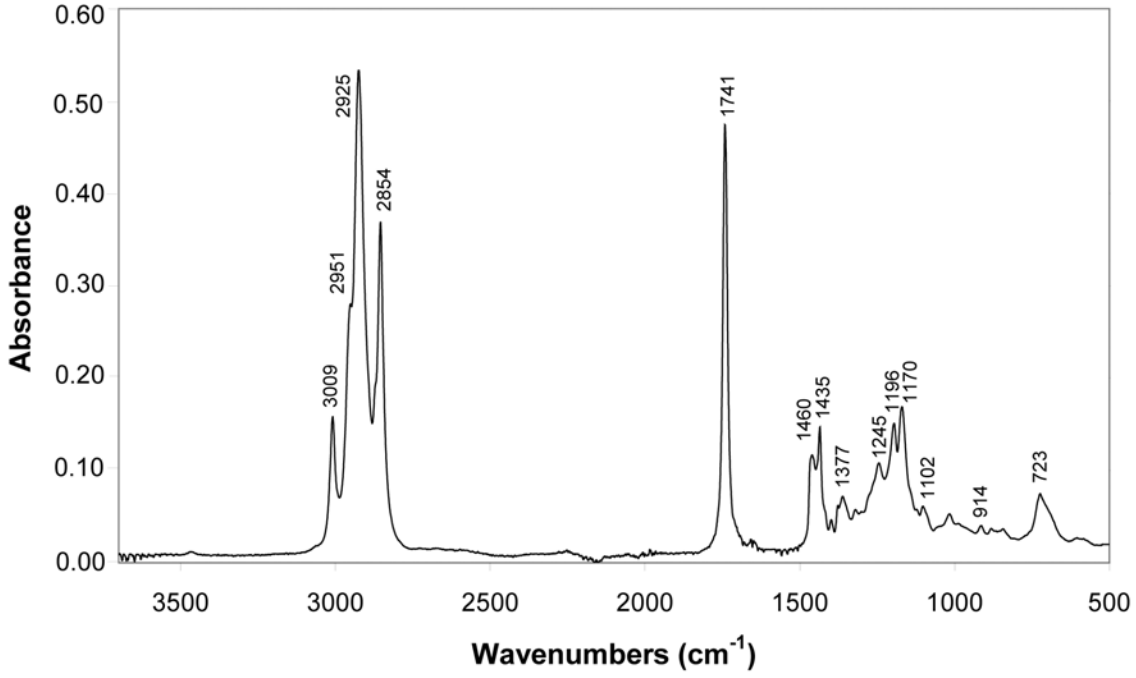

Figure 3.6 ATR spectrum of methyl linoleate acquired at room temperature.

The distinguishing features of the methyl stearate spectrum are that it contains no peaks above 3000 cm^{-1}, indicating the absence of C=C bonds. Peaks at 1169 cm^{-1} (C-O stretch in esters) and 719 cm^{-1} (CH_2 rocking vibration) are prominent. Methyl oleate contains a characteristic unsaturated C-H stretching band at 3004 cm^{-1} arising from the single C=C

bond in its alkyl chain. The analogous bands in methyl linoleate and methyl linolenate occur at slightly higher wavenumber (3009 cm^{-1} and 3010 cm^{-1} respectively).

Table 3.3 Peak assignments for methyl stearate, methyl oleate, methyl linoleate and methyl linolenate ATR spectra acquired at room temperature.[27, 28]

Peak (cm^{-1})				Assignment
Methyl Stearate	**Methyl Oleate**	**Methyl Linoleate**	**Methyl Linolenate**	
-	3004	3009	3010	νC-H (unsaturated)
2952	-	2951	2961	νC-H in $–CH_3$ (asym.)
2916	2922	2925	2927	νC-H in $–CH_2$- (asym.)
2870	-	-	-	νC-H in $–CH_3$ (sym.)
2848	2853	2854	2854	νC-H in $–CH_2$- (sym.)
1739	1742	1741	1740	νC=O (esters)
1462	1462	1460	1461	γC-H in CH_2/CH_3
1435	1435	1435	1435	
1381	-	-	-	-CH_3 sym. deformation
-	1377	1377	1360	
-	1244	1245	1245	νC-O (esters)
-	1196	1196	1196	
1169	1170	1170	1170	
-	1120	-	-	
-	-	1102	1104	
-	1094	-	-	
-	-	914	915	γC-H in $RCH=CH_2$
719	723	723	715	CH_2 rocking; γC-H in *cis* C=C

ν = stretching; γ = out-of-plane deformation

asym. = asymmetrical; sym. = symmetrical

The band at ~ 723 cm^{-1}, attributed to the CH_2 rocking vibration in methyl stearate, is increasingly more intense for the unsaturated methyl esters. This is due to a contribution from the *cis* C=C-H out-of-plane deformation band, which occurs at the same wavenumber.[6, 27] All four esters show the characteristic ester C=O stretching band at ~ 1740 cm^{-1}, however the precise position of this band is sensitive to the chemical environment of the carbonyl group.[27] The four methyl ester samples can therefore be readily distinguished by the characteristics of the C=O stretching band at ~ 1740 cm^{-1} and the unsaturated C-H stretching band just above 3000 cm^{-1}. These bands can also be monitored during ester thermo-oxidative decomposition to detect changes to C=C bonds in the ester alkyl chain and the formation of radical recombination and secondary oxidation products.[6, 9]

Figures 3.7A and 3.7B show the ATR spectra obtained for thermo-oxidatively decomposed methyl stearate, methyl oleate and methyl linoleate in the temperature range 100-350 ^oC in the C=O (1820-1550 cm^{-1}, figure 3.7A) and C-H (3050-2750 cm^{-1}, figure 3.7B) stretching regions. The spectra acquired for methyl linolenate are analogous to those of methyl linoleate.

For the methyl stearate, a gradual decrease in spectral intensity is observed until 200 ^oC, indicating that sample evaporation dominates the mass loss process below this temperature. Between 175 ^oC and 200 ^oC, chemical changes in the sample become evident. The CH_2 symmetrical and asymmetrical stretching bands at 2916 cm^{-1} and 2828 cm^{-1} and the C=O stretching band at 1739 cm^{-1} are shifted to higher wavenumber, suggesting thermal cracking of the ester hydrocarbon chain to form short chain hydrocarbons and carbonaceous deposits.[23] At 220 ^oC, bands at 1723 cm^{-1} and 3400 cm^{-1} appear. Although the 3400 cm^{-1} band could be a C=O stretching band overtone,[9] its high intensity implies the build up of hydroxyl species. These changes reveal the decomposition of methyl stearate into its alcoholic and carboxylic acid components which are subsequently volatilised.

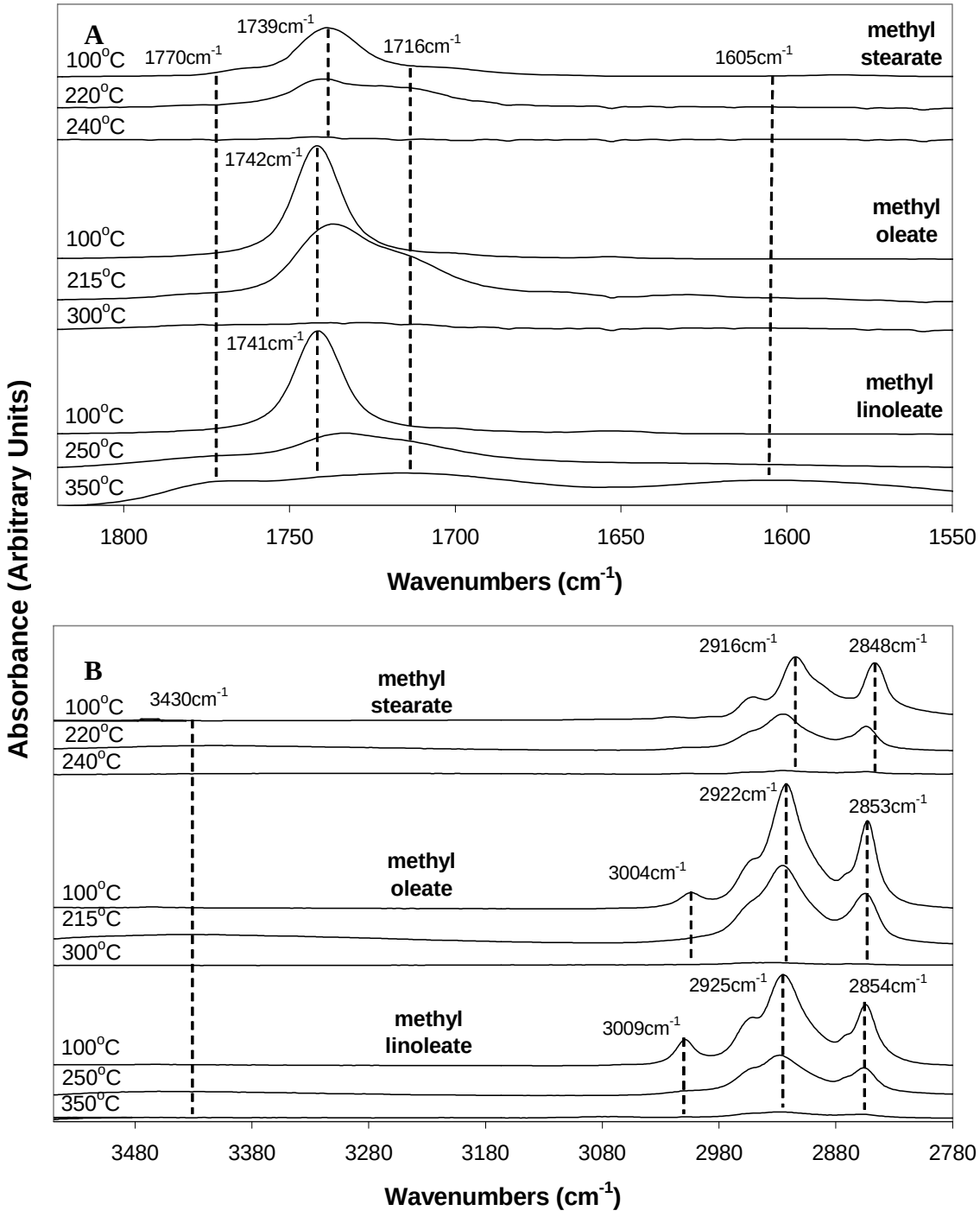

Figure 3.7 ATR spectra of thermo-oxidatively decomposed methyl stearate, methyl oleate and methyl linoleate samples in the region 1820-1550 cm^{-1} (A) and 3500-2780 cm^{-1} (B).

At 240 ^{o}C very little hydrocarbon-based material remains and the decomposition of the sample is essentially complete at higher temperatures. The temperature at which methyl stearate thermally decomposes by ATR (~ 200 ^{o}C) corresponds approximately to the TGA peak maximum temperature and the PDSC onset temperature of oxidation (both 207 ^{o}C). This confirms that the change in rate of mass loss observed after the TGA peak temperature represents a change in the volatilisation mechanism from evaporation to thermal decomposition.

The methyl oleate ATR results evidence an entirely different decomposition process to that observed for methyl stearate. Minimal sample evaporation is apparent at low temperatures and at 200 ^{o}C a broad OH stretching band at 3426 cm^{-1} is evolved, corresponding to the commencement of sample oxidation via hydroperoxide formation.[6] At 215 ^{o}C this band increases in intensity and shifts to higher wavenumber. Significant broadening of the C=O stretching band at ~ 1742 cm^{-1} and the evolution of bands at lower wavenumber (~ 1716 cm^{-1}) are also apparent. These changes infer that the radical species formed by hydroperoxide decomposition have undergone side reactions yielding volatile secondary oxidation products such as aldehydes, ketones and acids.[6, 9] Decomposition of the hydroperoxide species is also noticeable by changes in the C-H stretching region. A shift in the C-H stretching bands at 2853 cm^{-1} and 2922 cm^{-1} to higher wavenumber confirms that volatile products have been formed, whilst the decreasing intensity of the peak at 3004 cm^{-1} indicates reactions between radical species and C=C bonds in the oleate alkyl chain.

The only significant difference in the spectrum at 250 ^{o}C is the disappearance of the OH stretching band at 3426 cm^{-1}, signalling the complete decomposition of hydroperoxides. The decrease in spectrum intensity between 250 ^{o}C and 300 ^{o}C suggests that the high molecular weight products formed by branching reactions and any remaining secondary oxidation products have been volatilised, most likely via the reactions outlined by schemes 1.18-1.20 in Chapter 1. The decomposition process for methyl oleate is complete by 350 ^{o}C.

The chemistry of the methyl oleate thermo-oxidative decomposition process observed by ATR validates the identity of mass loss and heat flow events observed by TGA and PDSC. The evolution of hydroperoxide species at 200 ^{o}C supports the finding that methyl oleate decomposes via an oxygen uptake mechanism and that oxygen uptake occurs after sample evaporation has commenced. The temperature at which hydroperoxide formation occurs corresponds approximately to the 188 ^{o}C exotherm observed by PDSC and to the TGA event 1 peak maximum, indicating a change from evaporation to oxidative decomposition. The complete consumption of C=C bonds in the methyl oleate alkyl chain at 215 ^{o}C and the continuing build up of carbonyl species are in agreement with findings made by PDSC; the exotherms at 202 ^{o}C and 221 ^{o}C result from radical addition reactions to alkyl chain C=C bonds and the side reactions of radical species respectively. The decrease in spectrum intensity between 250 ^{o}C and 300 ^{o}C over the hydrocarbon and carbonyl regions suggests that the 259 ^{o}C event 2 shoulder observed by TGA corresponds to the degradation and volatilisation of high molecular weight deposits. Accordingly, reactions giving rise to these degradation processes are signified by the 'tail-like' region of the PDSC thermogram. The temperature at which the thermo-oxidative decomposition of methyl oleate is complete is similar to that obtained by TGA (~ 350 ^{o}C) and the ATR results confirm that no significant residues remain at higher temperatures.

The thermo-oxidative decomposition processes undergone by methyl linoleate and linolenate were analogous, although the observed changes occurred at lower temperatures for methyl linolenate due to its increased susceptibility to oxidation. Hence, this discussion will focus only on the results obtained for methyl linoleate.

In comparison to methyl stearate and methyl oleate, methyl linoleate undergoes very little evaporation at low temperatures. The first chemical change occurs at ~ 180 ^{o}C, 20 ^{o}C lower than for methyl oleate, whereby the build up of hydroxyl species is evidenced by the emergence of a broad band at 3460 cm^{-1}. A decrease in the unsaturated C-H stretching band intensity also occurs at this temperature, corresponding to radical addition reactions and the formation of high molecular weight material. The fact that the

consumption of C=C bonds takes place in conjunction with the evolution of hydroperoxides is testament to the higher reactivity of conjugated C=C bonds towards radical addition. It supports the findings made by Oyman et al.[6] that radical species are likely to add directly to conjugated C=C bonds. Changes in the C=O stretching region also occur at 180 ^{o}C; the band at ~ 1741 cm^{-1} broadens and a new band at ~ 1716 cm^{-1} appears, demonstrating the formation of volatile secondary oxidation products such as aldehydes, ketones and acids.[9]

At 200 ^{o}C hydroperoxides continue to be produced, however the intensity of the band at 3009 cm^{-1} is negligible, indicating that the consumption of C=C bonds is almost complete. Carbonyl-type compounds continue to be evolved and further decreases in spectral intensity indicate the loss of volatiles. The O-H and unsaturated C-H stretching bands have disappeared at 250 ^{o}C such that hydroperoxide species have been fully decomposed and the consumption of C=C bonds is complete. The intensity of the C-H stretching bands continues to decrease as a result of thermal degradation. At temperatures above 250 ^{o}C, the decomposition processes undergone by methyl linoleate are more complex than those observed for methyl stearate and methyl oleate. A broad band at 1770 cm^{-1} appears at 300 ^{o}C, suggesting the formation of C-O-C and C-O-O-C linkages (see scheme 1.15 in Chapter 1) via radical recombination reactions.[6] This band, together with the band at 1716 cm^{-1}, increases in intensity up until 350 ^{o}C and implies that a high concentration of radical species must be present in the methyl linoleate sample after all C=C bonds have been consumed.[6] A band at 1605 cm^{-1} also becomes apparent at 350 ^{o}C. This band is characteristic of metal carboxylates or 'soaps'[29] and represents the reaction of carbonyl compounds such as acids with the aluminium pan surface (scheme 3.4).

$$2R-COOH + Al_2O_3 \rightarrow R-COO_2Al_2O_2 + H_2O$$

Scheme 3.4 Reaction between carboxyl compounds and aluminium oxide to form aluminium carboxylates and water.

The formation of these complexes was not observed for methyl stearate or methyl oleate as a result of the complete volatilisation of these esters by 350 ^{o}C.

The combustion of hydrocarbon-based material is not complete until ~ 400 ^{o}C for methyl linoleate, indicating the significant thermal stability of the high molecular weight residues formed. The carboxylate residue and radical recombination products persist up to 500 ^{o}C so that it is these products, and not the thermally stable crosslinked networks formed by the oxidative decomposition of the methyl linoleate sample, that comprise the high levels of residue present at temperatures of 500 ^{o}C and above. Given that metal soaps have long been associated with metallic coating problems,[30, 31] this reveals that the products formed by the oxidative decomposition of highly unsaturated esters can potentially give rise to uncoated defects.

As for methyl stearate and methyl oleate, the chemical changes observed by ATR during the thermo-oxidative decomposition of methyl linoleate verify findings made by TGA and PDSC. The build up of hydroperoxides at 180 ^{o}C, together with the reactions of radical species with the C=C bonds and evolution of volatile secondary oxidation products correspond to the TGA event 1 peak temperature (186 ^{o}C). As was noted for methyl oleate, due to the high oxygen pressures employed during PDSC testing, the oxidation onset temperature measured by PDSC (136 ^{o}C) is considerably lower than the temperature at which oxidation reactions commence by ATR. The fact that C=C bonds present in the linoleate alkyl chain are almost completely consumed by 200 ^{o}C and that the evolution of volatile carbonyl compounds continues up to higher temperatures confirms that the PDSC exotherm at 226 ^{o}C represents radical side reactions. The decrease in the C-H stretching region intensity from ~ 250 ^{o}C corresponds to the 260 ^{o}C event 2 peak temperature measured by TGA and the initiation of thermal decomposition reactions. Radical recombination reactions were found to occur at ~ 300 ^{o}C. These reactions, together with the decomposition of high molecular weight networked material and the formation of metal carboxylates, are unique to conjugated methyl esters and give rise to the numerous events observed within the secondary decomposition regions by TGA and PDSC.

3.1.4 Conclusions

TGA and PDSC techniques have been coupled with chemical characterisation by ATR to study the thermo-oxidative decomposition and residue formation processes undergone by four methyl esters of varying levels of alkyl chain unsaturation. The results show that increasing the number of C=C bonds in the ester alkyl chain produces greater amounts of thermally stable residue as determined by the % B/A ratio technique.[7, 8] The residues formed during the decomposition of more saturated esters (methyl stearate and methyl oleate) comprise of linear and branched hydrocarbon material. This material is completely decomposed at temperatures below 500 ^{o}C. In contrast, the decomposition residues formed by polyunsaturated methyl esters are not strictly 'carbonaceous' in nature. They comprise of metal carboxylates and radical recombination reaction products which persist to temperatures above 500 ^{o}C. Given this, the use of highly unsaturated esters in industrial lubricants is likely to result in the formation of high levels of residual deposits which have the potential to cause significant problems in the metallic coatings industry.

3.2 Consequences of Residue Formation from Triglyceride and Commercial Base Ester Thermo-Oxidative Decomposition for 55Al-43.4Zn-1.6Si Coating Quality

3.2.1 Introduction

Triglyceride-based fats and oils are exploited by a range of different industries and their use within oil formulations applied during the cold rolling of sheet steel is prevalent.[30, 32-34] Modern cold rolling oils typically constitute between 20 and 90 percent by mass of triglycerides blended with semi-synthetic and/or synthetic poly-functional ester derivatives.[30] It is the properties of these blends which make them ideal for use in metal working applications. Unlike mineral oils, triglycerides and other poly-functional esters possess low pressure-viscosity coefficients, enabling them to remain fluid at the high pressures employed during cold rolling and to accommodate the fresh metal surfaces

created by the reduction process.[32] Given that rolling oils are subject to high (~ 250 ^{o}C) temperatures during cold rolling, the esters used must also possess excellent resistance to oxidative and thermal degradation. The use of triglyceride/semi-synthetic/synthetic ester blends, as opposed to neat triglycerides, flows from these requirements; in the absence of anti-oxidants, synthetic and semi-synthetic esters possess superior thermal, oxidative and hydrolytic stability.[10, 32, 35] However, the oil film left on the steel surface after cold rolling must be completely removed prior to the application of a metallic coating. Since oil removal is commonly achieved by treating the steel in a furnace, the esters used in cold rolling oil formulations must also be capable of volatilising at high (≥ 500 ^{o}C) temperatures without leaving thermally stable residues; deposits remaining on the steel surface after furnace treatment have been associated with the formation of pinhole uncoated and mini-spangle defects in metallic coatings.[36-38] In light of these complicated - and often competing - requirements, the selection of appropriate base esters for use within cold rolling oil formulations is critical.

The chemical structure of a representative triglyceride containing three different fatty acid chains is given in scheme 3.5.

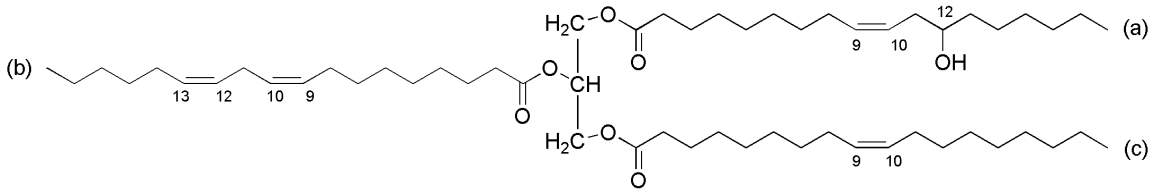

Scheme 3.5 Representation of a typical triglyceride containing (a) ricinoleic acid, (b) linoleic acid and (c) oleic acid moieties.

The chemical structure and distribution of the fatty acid alkyl chains contained in triglycerides obtained from different sources vary significantly, and are determinative of physical state, thermal and oxidative stability and lubricity.[1] Variations can be found in fatty acid carbon chain length, degree of unsaturation and the presence of unique functionalities such as hydroxyl groups.

Wet chemistry and spectroscopic techniques have been used extensively to study both the chemistry of rolling oil films remaining on the steel surface after the cold rolling process and the nature of the products formed by the low temperature decomposition of triglycerides, semi-synthetic and fully-synthetic esters.[29, 39-41] However, little has been done to comprehensively characterise the volatile and residual decomposition products formed during the furnace cleaning process and the dependency of these products on ester chemical structure.[42, 43] In addition, the majority of studies have focussed on oil decomposition under reducing atmospheres (hydrogen or hydrogen/nitrogen gas mixtures);[23, 24, 33] less in known about oil thermo-oxidative decomposition.

The use of thermal analysis techniques such as TGA and PDSC to characterise the thermal and oxidative stability base esters is well-documented.[2, 4, 5, 10, 19, 20, 33, 42, 44, 45] However, most studies have been directed towards the determination of oxidative stability as measured by oxidation induction time and various kinetic parameters.[5, 10, 19, 20, 44-46] Several groups have studied the triglyceride thermo-oxidative decomposition process under ramped heating conditions and up to high ($\geq 500\ ^{o}C$) temperatures.[4, 5, 7, 8] However, the decomposition events observed have not been assigned to specific chemical processes and the identity of residues remaining at different stages during base ester thermo-oxidative decomposition is unknown. Furthermore, the impact of residue on the quality of metallic coatings subsequently placed onto the steel surface is poorly understood and no comprehensive study has been undertaken to determine whether varying the chemical structure of base ester fatty acid alkyl chains can eliminate or reduce residue levels.

This work seeks to resolve some of the above issues by investigating the effect of fatty acid chemical structure (unsaturation levels, chain length distribution and the presence of an hydroxyl functionality) on the thermo-oxidative decomposition of seven naturally occurring triglycerides and one fully-synthetic/two semi-synthetic commercial base esters by TGA, PDSC and ATR techniques. Hydrogenated derivatives of several of the esters have also been synthesised and analysed by TGA and PDSC to contrast the thermo-oxidative decomposition processes undergone by unsaturated/completely

saturated esters. Furthermore, the thermo-reductive decomposition processes undergone by the esters are analysed under a 5 % hydrogen-95% nitrogen (HNX) gas mixture to reveal the dependency of residue levels on ester molecular weight and chain length distribution and to simulate an alternative furnace environment to that employed during continuous annealing. Relationships between ester chemical structure and 55Al-43.4Zn-1.6Si hot dip metallic coating quality have also been elucidated by performing industrial-scale hot dipping trials and experimental hot dipping simulations.

3.2.2 Experimental

3.2.2.1 Sample Preparation

3.2.2.1.1 Materials

A list of materials, which were used without further purification, is given in table 3.4. The seven triglycerides analysed, coconut oil, palm oil, castor oil, sesame oil, cottonseed oil, safflower oil and canola oil, originate from commonly known vegetable sources and were selected due to systematic variations in the chain length and levels of unsaturation in their alkyl chains. Castor oil was included as a result of its unique alkyl chain composition; it consists of roughly 89 % ricinoleic acid, a fatty acid that contains a 9,10 double bond and an OH group in the C-12 position. The alkyl chain compositions of the triglycerides together with their percentages by mass of polyunsaturated, monounsaturated and saturated alkyl chains are summarised in table 1.3 in Chapter 1.

Commercial base esters A and C are semi-synthetic derivatives produced by the trans-esterification of coconut oil with a tri-functional (ester A) or di-functional (ester B) polyol (refer to scheme 1.4 in Chapter 1). Ester B is a fully-synthetic product synthesised from the same tri-functional alcohol as ester A and oleic acid. All triglyceride and commercial base ester samples were kept in the dark and under nitrogen to minimise oxidation during storage.

The properties of the other materials used are described in Chapter 2 as follows:

- cold rolled steel - table 2.3;

- 55Al-43.4Zn-1.6Si alloy - table 2.4;
- shellite solvent - section 2.2.5;
- oxygen and HNX gases - section 2.2.6, and
- TGA and PDSC consumables - section 2.2.7.

Table 3.4 Summary of materials used in Chapter 3.2.

Compound	Source	Purity
Coconut oil	Quaker Chemical	-
Canola oil	Supelco (Bellefonte, Pennsylvania)	neat
Palm oil		
Safflower oil		
Sesame oil	Sigma-Aldrich Australia (Castle Hill, New South Wales)	neat
Cottonseed oil		
Castor oil	ACE Chemicals (Adelaide, South Australia)	-
Ester A	Quaker Chemical	-
Ester B		
Ester C		
Chloroform	Ajax Finechem (Seven Hills, New South Wales)	AnaLaR
Chloroform-D + silver foil	Cambridge Isotope Laboratories, Inc. (Andover, Massachusetts)	99.8 %
Ethanol	Ajax Finechem (Seven Hills, New South Wales)	AnaLaR
10 % Pd-C catalyst	Sigma-Aldrich Australia (Castle Hill, New South Wales)	9.8 – 10.2 % Pd
Celite	-	-

3.2.2.1.2 Hydrogenation

Hydrogenation was used to create saturated analogues of sesame and cottonseed oils and the commercial base esters to enable identification of the mass loss (TGA) and heat flow (PDSC) events corresponding to the reactions of C=C bonds. A Parr High Pressure Hydrogenator was used to carry out all hydrogenation reactions. The ester sample (2-8

g) was dissolved in ethanol (200 ml) in a 500 ml Parr reaction vessel. 10 % (w/w) palladium on activated carbon (10 % Pd-C) catalyst (0.6-2.0 g) was added and the reaction vessel was loaded into the hydrogenator. The vessel was then evacuated and purged three times with high purity hydrogen gas (BOC Gases Australia) before being filled to a pressure of 40 psi. The reaction vessel was agitated for 4 hours to ensure the complete reaction of C=C bonds in the sample. After hydrogenation, liquid reaction products were filtered over Celite to remove the catalyst before being dried under vacuum. Solid reaction products were extracted into chloroform (100 ml) prior to filtration.

3.2.2.1.3 Sample Preparation for ATR

Representative triglyceride and commercial base ester samples were prepared for mid-infrared ATR analysis according to the procedure described in Chapter 2 (refer to section 2.3.2).

3.2.2.1.4 Preparation of 55Al-43.4Zn-1.6Si Coated Steel Samples

55Al-43.4Zn-1.6Si hot dip metal-coated samples were prepared using representative triglyceride and commercial base ester samples according to the hot dip simulation and industrial hot dipping trial procedures described in Chapter 2 (refer to sections 2.3.3 and 2.3.4 respectively).

3.2.2.2 Characterisation of Hydrogenated Esters

3.2.2.2.1 Nuclear Magnetic Resonance (NMR)

NMR spectroscopy was used to analyse both the non-hydrogenated and hydrogenated ester samples to confirm the consumption of C=C bonds. The ester (~ 5 mg solid or 50 μL liquid) was dissolved in deuterated chloroform (~ 1 mL) for analysis. ^{1}H spectra were recorded on a Varian Gemini FT-NMR liquid nitrogen-cooled 300 MHz spectrometer. Spectral analysis was performed using VNMR 6.1 analysis software. The chemical shifts are reported in ppm downfield from trimethylsilane.

3.2.2.3 Characterisation of Thermal Decomposition Behaviour

3.2.2.3.1 TGA

The thermo-oxidative decomposition profiles of the triglycerides, commercial base esters and hydrogenated ester derivatives and the thermo-reductive decomposition profiles of the triglycerides and commercial base esters were analysed by TGA under oxygen and HNX respectively according to the conditions and procedure described in Chapter 2 (refer to section 2.4.1).

3.2.2.3.2 PDSC

The triglyceride, commercial base ester and hydrogenated ester samples were analysed by PDSC according to the conditions and procedure described in Chapter 2 (refer to section 2.4.2).

3.2.2.3.3 ATR

ATR analysis of the triglycerides and commercial base esters was undertaken according to the mid-infrared analysis method detailed in Chapter 2 (refer to section 2.4.3).

3.2.2.4 Characterisation of 55Al-43.4Zn-1.6Si Coating Quality

3.2.2.4.1 Industrial Hot Dipping Trial Samples

55Al-43.4Zn-1.6Si coated samples prepared using the industrial hot dipping trial procedure were visually assessed and analysed by optical microscopy and Scanning Electron Microscopy (SEM) according to the methods described in Chapter 2 (refer to section 2.4.5).

3.2.2.4.2 Hot Dip Simulation Samples

55Al-43.4Zn-1.6Si coated samples prepared using the hot dip simulation procedure were analysed by optical microscopy and the % uncoated defect area for each sample was calculated according to the method described in Chapter 2 (refer to section 2.4.4.1).

3.2.3 Results and Discussion

3.2.3.1 Thermo-Oxidative Decomposition Profile by TGA

3.2.3.1.1 Triglycerides

TGA analysis was performed on seven triglycerides to study the effect of variations in fatty acid chain chemical structure of the thermo-oxidative decomposition process. Figure 3.8 shows a typical TGA thermogram obtained for coconut oil. Both the TG and DTG curves are shown.

The thermo-oxidative decomposition of coconut oil is similar to that of a polyunsaturated methyl ester and contains three mass loss events. The onset temperature of mass loss occurs at an average of 231 ^{o}C, a value which is higher than that obtained for any of the other triglycerides or for the methyl esters studied in 3.1. This increased thermal stability and resistance to oxidative decomposition is due to coconut oil's high level of saturated alkyl chains (in comparison to the other triglycerides)[1, 20] and to the higher molecular weight of the triglyceride molecule (in comparison to methyl esters).[10]

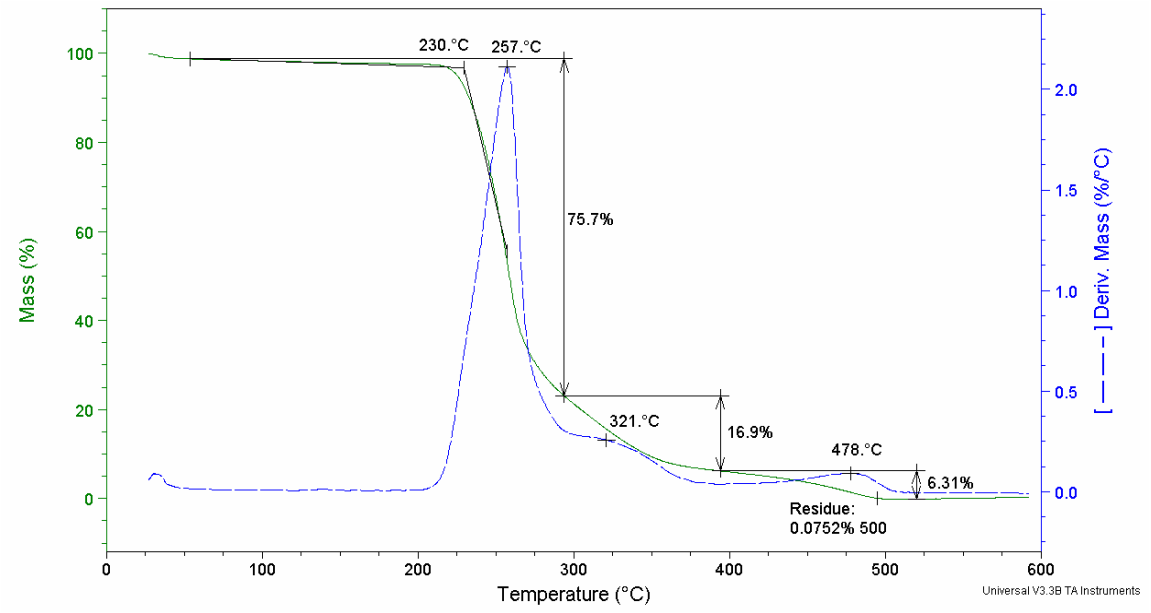

Figure 3.8 Coconut oil thermo-oxidative decomposition profile by TGA.

The primary decomposition region (room temperature-300 ^{o}C) for coconut oil contains a single DTG curve mass loss peak at 256 ^{o}C, whilst the secondary decomposition region (300-530 ^{o}C) consists of two events at 323 ^{o}C and 477 ^{o}C. It should be noted that the percentage of sample mass lost over the primary and secondary regions is not equivalent to either the percentage of saturated and unsaturated alkyl chains or the loss of the constituent functional components of the triglyceride molecule. This observation applies to all of the triglycerides studied and whilst it is consistent with the findings of Vora et al.[47] it contradicts those of Santos et al.,[5] who postulated that the three thermo-oxidative decomposition events observed for a range of triglycerides represented the decomposition of polyunsaturated, monounsaturated and saturated fatty acid components respectively. There is no initial mass increase corresponding to oxygen uptake for coconut oil due to its high level of saturation.

The thermo-oxidative decomposition of palm, cottonseed, sesame, canola and safflower oils is similar to that of coconut oil, although as many as five mass loss events are observed for these samples. Castor oil displays a unique thermo-oxidative decomposition profile that will be discussed separately. Figure 3.9 shows a comparison between the DTG curves obtained for the triglycerides. The five decomposition events are labelled as 1-5 on each curve. Table 3.5 presents the onset points (T_{onset}), peak and shoulder temperatures (T_{max}) and corresponding mass losses for the triglycerides.

Cottonseed, sesame, canola and safflower oil all undergo a mass increase corresponding to oxygen uptake prior to volatilisation, indicating that mass loss in these triglycerides is initiated by hydroperoxide formation (schemes 1.10-1.11 in Chapter 1).[2, 3, 5, 6, 17, 18] The amount of oxygen absorbed increases with increasing levels of alkyl chain unsaturation and triglycerides such as safflower oil which are high in polyunsaturated alkyl chains display a proportionally greater mass increase than those containing monounsaturates. Oxygen uptake is not observed for coconut or palm oils; high levels of saturated alkyl chains result in greater resistance to oxidation so that oxygen uptake occurs simultaneously with mass loss processes such as evaporation.

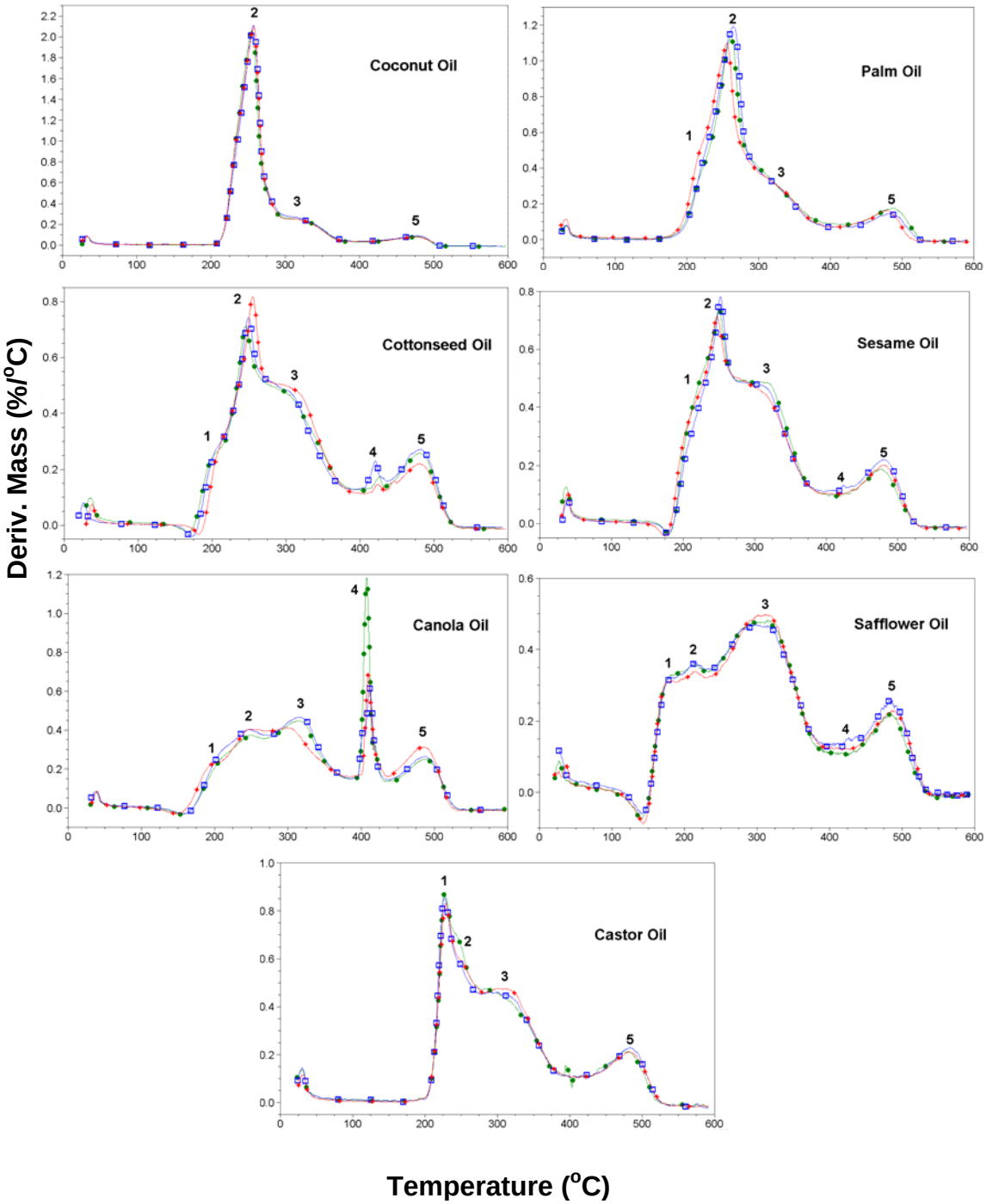

Figure 3.9 Overlays of TGA thermo-oxidative decomposition profiles (DTG curves) for the seven triglycerides.

Table 3.5 Summary of TGA thermo-oxidative decomposition data for the seven triglycerides. Errors are less than ± 5 % except for the % residue at 500 °C (± 20 %).

Triglyceride	T_{onset} (°C)	O_2 Uptake (%)	T_{max} Event 1 (°C)	Mass Loss Event 1 (%)	T_{max} Event 2 (°C)	Mass Loss Event 2 (%)	T_{max} Event 3 (°C)	Mass Loss Event 3 (%)	T_{max} Event 4 (°C)	Mass Loss Event 4 (%)	T_{max} Event 5 (°C)	Mass Loss Event 5 (%)	% Residue at 500 °C
Coconut Oil	231	-	-	-	256	76.7	323	15.2	-	-	477	5.89	1.7
Palm Oil	221	-	222	13.6	261	45.0	312	26.5	-	-	482	11.7	3.6
Cottonseed Oil	212	0.50	208	7.20	250	29.2	302	41.7	424	5.93	481	14.2	4.3
Sesame Oil	211	0.55	215	12.8	250	27.4	306	41.1	426	3.77	479	10.8	4.3
Canola Oil	195	0.82	205	8.97	248	18.5	309	36.2	410	15.9	486	16.7	7.9
Safflower Oil	173	1.6	183	10.2	214	13.4	305	59.4	-	-	485	18.1	4.5
Castor Oil	212	-	228	21.0	247	19.6	299	39.1	-	-	482	17.1	5.2

The onset temperatures of mass loss for the triglycerides range from 173-231 ^{o}C. These values are comparable to those reported by Coni et al.[2] for a series of highly unsaturated oils analysed under oxygen. The thermo-oxidative stability of the triglycerides generally increases with increasing saturated alkyl chain content and the order of the triglycerides (except castor oil) with respect to increasing thermal stability is safflower oil < canola oil < sesame oil < cottonseed oil < palm oil < coconut oil. There are, however, several inconsistencies in this trend. Despite safflower oil containing a marginally lower total amount of unsaturated alkyl chains than canola oil (90.8 % w/w as opposed to 92.2 % w/w respectively), safflower oil displays a lower onset temperature. Furthermore, the onset temperatures of sesame and cottonseed oils are virtually the same despite sesame oil containing a higher total percentage of unsaturated alkyl chains (84.9 % w/w as opposed to 71.9 % w/w in cottonseed oil). This is in accordance with the findings of Oyman et al.[6] and verifies the observations made with respect to oxygen uptake by suggesting that triglycerides containing high levels of polyunsaturated alkyl chains are less stable towards thermo-oxidative decomposition. Santos et al.[5] arrived at a different conclusion; they found sunflower oil, which is high in polyunsaturates, to be more thermally stable than olive oil, which is high in monounsaturates. However, their investigation was performed under an atmosphere of air so that triglyceride molecular weight, and thus the distribution of alkyl chains of different lengths, would play a greater role in determining oil thermal stability than it would under an oxygen atmosphere alone.

The primary thermo-oxidative decomposition region for all triglycerides except coconut oil contains two mass loss events, the first occurring at an average value of 210 ^{o}C (event 1) and the second at 247 ^{o}C (event 2). The proportions of events 1 and 2 vary between the triglycerides and are linked (although not directly proportional) to the level and type of unsaturated alkyl chain constituents. Figure 3.10 shows the percentage of sample mass lost over each of the five events for the seven triglycerides. Although there is no distinct trend between triglyceride unsaturation levels and the proportion of sample mass lost over event 1 (~ 210 ^{o}C), triglycerides containing high levels of

monounsaturated alkyl chains lose a greater amount of mass than their polyunsaturated counterparts. In addition, event 1 is almost undetectable in coconut oil, which comprises 92.0 % w/w saturated alkyl chains. In light of these observations and the general reaction processes undergone by fats and oils during oxidation (refer to schemes 1.9-1.16 in Chapter 1), event 1 represents the formation of hydroperoxide species following oxygen uptake by the triglyceride samples and subsequent hydroperoxide decomposition to produce radicals such as R•, RO•, ROO• and •OH.[5, 6, 17, 18] Although a small amount of sample evaporation may also be occurring, the low levels of event 1 mass loss observed for both unsaturated and saturated triglycerides suggest that the processes responsible for mass loss do not evolve significant amounts of volatiles.

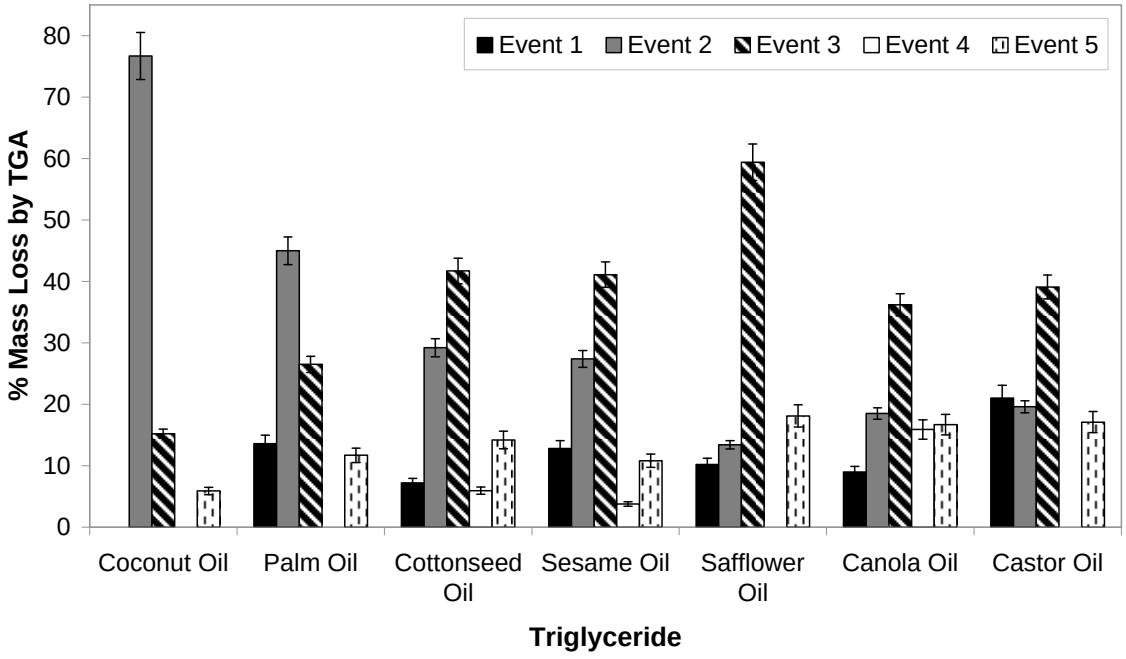

Figure 3.10 Percentage mass lost over each of the five TGA events observed during the thermo-oxidative decomposition of the triglycerides. The error bars represent ± 5 % error.

In contrast to event 1, the proportion of mass loss during event 2 (~ 247 ^{o}C) is significantly higher for saturated triglycerides such as coconut oil, indicating that event

2 predominantly represents triglyceride evaporation. The fact that the more highly unsaturated triglycerides undergo less evaporation/mass loss over event 2 can be rationalised by considering the reactions of radical species formed during event 1. Radicals can participate in three competing reaction routes; propagation via addition to C=C bonds present in unsaturated ester alkyl chains (depicted by scheme 3.3 above and scheme 1.14 in Chapter 1), termination via radical recombination reactions (scheme 1.15 in Chapter 1) and secondary oxidation leading to the evolution of volatiles (scheme 1.16 in Chapter 1).[6, 18] The probability of radical recombination is small as a result of the low initial concentration radical species in the triglycerides; the ramped heating conditions and limited triglyceride exposure to the catalytic aluminium pan surface reduce the rate of oxidation initiation.[6] Given this, the thermo-oxidative decomposition of the triglycerides involves a balance between the formation of non-volatile, high molecular weight crosslinked deposits by radical addition reactions and the evolution of volatiles via evaporation and secondary oxidation.

In highly saturated triglycerides such as coconut oil, comparatively few C=C bonds are available for reaction with radicals, limiting the formation of crosslinked deposits. Radicals are therefore more likely to decompose via secondary oxidation pathways, producing volatile aldehydes, short-chain esters, alkanes and carboxylic acids and carbon dioxide.[6, 18] Furthermore, a significant proportion of triglyceride molecules are able to undergo evaporation as a result of limited crosslinking. Therefore in highly saturated triglycerides, significant levels of sample mass loss occur during event 2 as a result of evaporation and secondary oxidation.

The greater concentration of C=C bonds present in unsaturated triglycerides results in more radical addition reactions and the formation of high molecular weight deposits, suppressing both triglyceride evaporation and the formation of volatiles via secondary oxidation reactions. The proportion of sample mass lost over event 2 therefore decreases with increasing levels of alkyl chain unsaturation.

Up to three mass loss events are observed in the triglyceride secondary decomposition region (300-500 ^{o}C). The first of these (event 3) occurs at ~ 308 ^{o}C, a temperature that is

~ 50 ^{o}C higher than the first secondary region event observed for methyl esters. The proportion of mass lost over event 3 increases with increasing levels of unsaturation and is particularly high for polyunsaturated triglycerides such as safflower oil. This implies that the dominant processes giving rise to event 3 mass loss are radical decomposition via secondary oxidation and the thermal cracking of branched and/or crosslinked material (scheme 1.18 in Chapter 1).[6, 18, 23, 48]

Following the complete consumption of C=C bonds present in the unsaturated triglyceride alkyl chains, high concentrations of high molecular weight material and unreacted radicals are present. The thermal cracking reactions undergone by the high molecular weight material result in the formation of both volatiles (short-chain hydrocarbons) and residues (carbonaceous deposits), giving rise to a modest amount of mass loss.[23, 48] Unreacted radicals can be destroyed by two reaction pathways; secondary oxidation or termination via recombination.[6, 18, 48] Given the high temperature and the limited mobility of radicals as a result of crosslinking, the most favourable radical reaction pathway is secondary oxidation, a process that results in significant amounts of mass loss.[6, 18] Since highly polyunsaturated triglycerides contain considerable amounts of both radicals and high molecular weight material, they undergo greater mass loss via secondary oxidation and thermal cracking during event 3.

Event 4 is a sharp peak in the DTG curve at ~ 420 ^{o}C and involves rapid sample mass loss. It is particularly prominent in the cottonseed and canola oil thermograms, however it is largely obscured by surrounding mass loss events for sesame and safflower oil and is undetectable for palm and coconut oil. The fast rate of mass loss over event 4 together with the fact that highly unsaturated triglycerides exhibit a greater amount of mass loss implies that event 4 represents the combustion of residual carbonaceous material remaining after thermal cracking during event 3 (scheme 1.19 in Chapter 1).

The final mass loss event within the secondary decomposition region (event 5) occurs at ~ 480 ^{o}C. Although this event results in a small proportion of sample mass loss, it is present in the TGA results of all the triglycerides and its magnitude increases with increasing unsaturation. The temperature at which event 5 occurs is similar to that

observed for the decomposition of radical recombination products and metal carboxylates formed in polyunsaturated methyl esters. These observations suggest that event 5 represents the thermal decomposition and/or volatilisation of persistent radical recombination and soap-like residues (scheme 1.6 in Chapter 1).[4]

Whilst the secondary decomposition region events undergone by castor oil are similar to those observed for the other triglycerides, its low temperature mass loss events are considerably different. Castor oil contains 89.0 % w/w ricinoleic acid, a monounsaturated fatty acid with a hydroxyl functional group in the C-12 position. It is more highly unsaturated than the other triglycerides, yet no oxygen uptake is observed prior to its thermo-oxidative decomposition. In addition, its onset temperature (212 ^{o}C), event 1 peak maximum temperature (228 ^{o}C) and event 1 mass loss (21.0 %) are comparatively high. These observations are consistent with the findings of Guttman and Odzeniak,[46] who determined that the activation energy associated with the oxidative decomposition of castor oil is greater than that of other highly unsaturated oils. Furthermore, given that castor oil is susceptible to polymerisation via hydroxyl group condensation,[1] event 1 involves the competition between such condensation reactions (scheme 3.6) and hydroperoxide decomposition, limiting the radical species available to form volatile secondary oxidation products and undergo crosslinking reactions in the castor oil sample.

Secondary oxidation products such as short-chain carboxylic acids and alcohols can also be consumed according to scheme 3.6. These factors rationalise both the high level of mass loss observed for castor oil over event 1 (the evolution of a large amount of water) and the relatively low proportion of mass loss over events 3 and 5 (limited amounts of high molecular weight material and radical recombination products are formed as a result of low concentrations of radical species). However, given that the levels of thermally stable residue present at 500 ^{o}C (5.2 %) are not significantly greater than for the other triglycerides, events 3 and 5 must account for the decomposition and volatilisation of the products formed by condensation reactions.

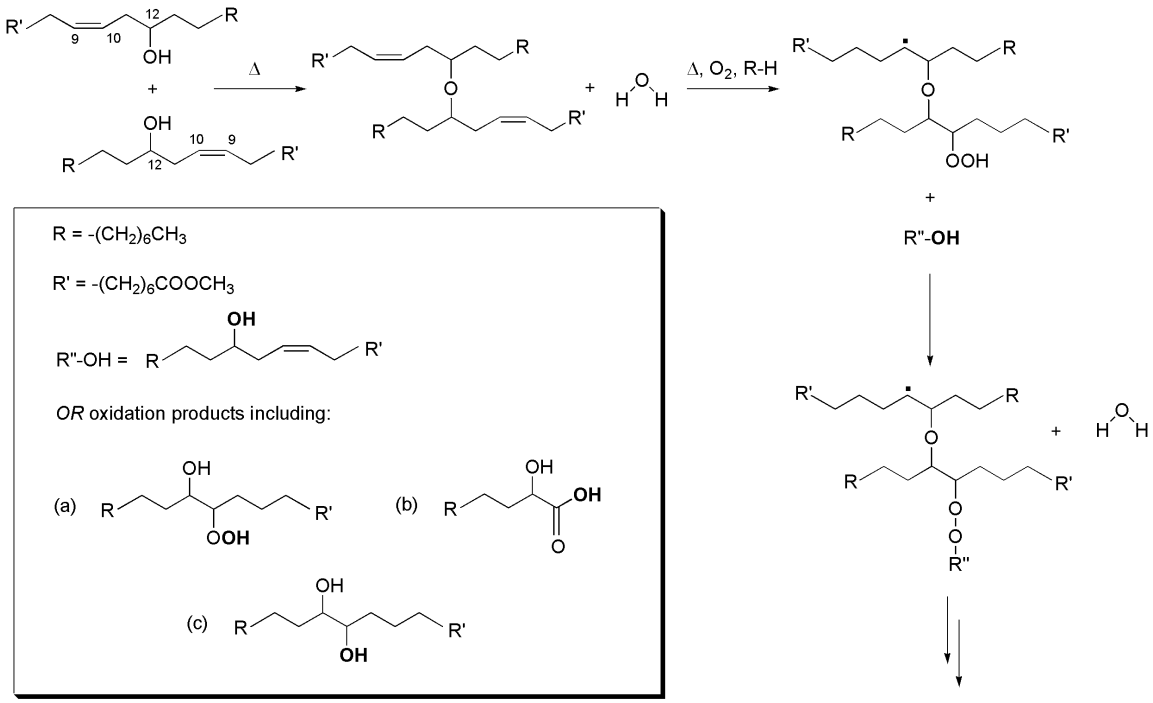

Scheme 3.6 Schematic representation of the condensation polymerisation and oxidative crosslinking reactions undergone by castor oil.

The temperature at which the thermo-oxidative decomposition of the triglycerides is complete (the decomposition end temperature, T_{end}) does not vary significantly between samples, occurring at 500-530 ^{o}C. Despite this, there is a general relationship between sample unsaturation and the temperature at which sample mass loss is complete such that samples containing higher levels of unsaturated alkyl chains display higher decomposition end temperatures: T_{end} coconut oil < palm oil < cottonseed oil = sesame oil < canola oil < safflower oil. As a consequence of the high end temperatures measured for the triglycerides, the % residues remaining at 500 ^{o}C are significantly greater than those measured for methyl esters (1.7-7.9 %, as opposed to < 1.0 % respectively). The % residue data shows an analogous trend to that observed between triglyceride unsaturation and decomposition end temperature; highly unsaturated triglycerides leave greater amounts of residue at 500 ^{o}C.

3.2.3.1.2 Commercial Base Esters

TGA analysis of commercial base esters A, B and C reveals a thermo-oxidative decomposition profile similar to that of the triglycerides. Figure 3.11 shows an overlay of the DTG curves obtained for the commercial esters and for coconut oil, the parent triglyceride of semi-synthetic esters A and C. Mass loss events are labelled as 1-5 and the onset points (T_{onset}), peak and shoulder temperatures (T_{max}) and the relevant mass losses are presented in table 3.6.

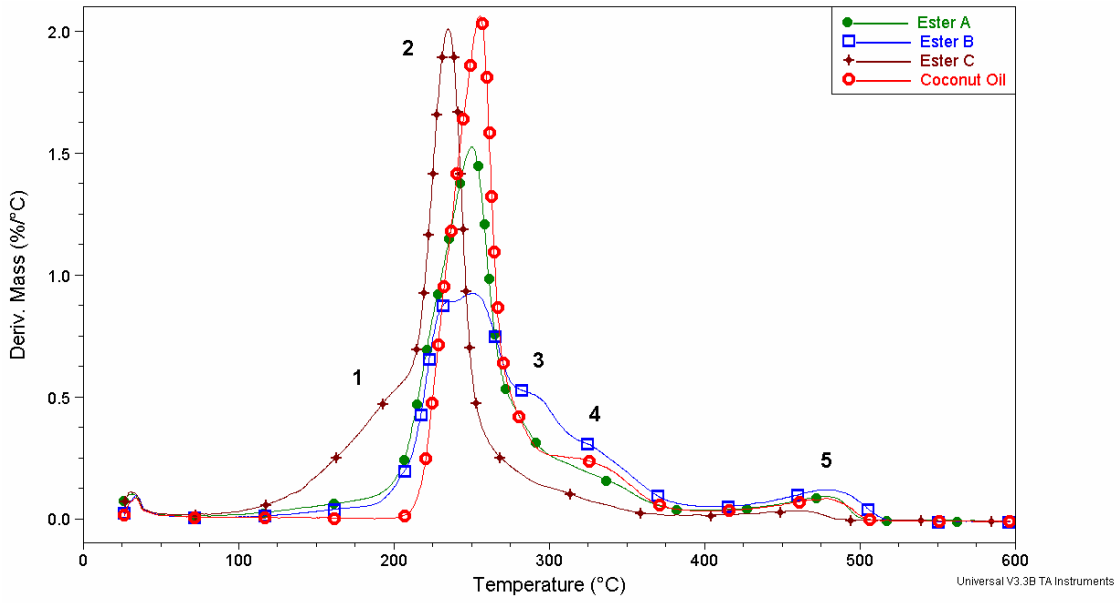

Figure 3.11 Overlay of the TGA thermo-oxidative decompositions profiles (DTG curves) of the three commercial base esters and coconut oil.

The commercial base ester thermo-oxidative decomposition process is similar to that of the triglycerides, with three mass loss events occurring over the primary decomposition region (room temperature-300 ^{o}C) and two over the secondary decomposition region (300-500^{o}C). Despite this, several notable differences are evident. The mass loss onset temperatures of all three commercial esters are lower than that of coconut oil. This verifies the findings of Gamlin et al.,[10] who concluded that a natural oil was more

resistant to oxidation than semi-synthetic or synthetic oils due to the presence of naturally-occurring anti-oxidants. As for the triglycerides, the commercial ester T_{onset} values are linked to alkyl chain unsaturation. The T_{onset} of ester B, which contains 100 % oleate alkyl chains, is ~ 5 ^{o}C lower than that of ester A, a semi-synthetic derivative of coconut oil. However, ester C's T_{onset} (199 ^{o}C) is below that of the other commercial esters and most of the triglycerides due to its low molecular weight; it is a di- as opposed to tri-ester.

Unlike the triglycerides, the commercial esters undergo a small amount of mass loss prior to the major mass loss event (event 2). This mass loss is represented by event 1, which occurs at ~ 174 ^{o}C in esters A and B and at 197 ^{o}C in ester C. Event 1 is likely to represent the volatilisation of free fatty acids together with mono- and di-esters contained in the commercial ester samples and precludes the observation of a mass increase corresponding to oxygen uptake.

Event 2 is the major mass loss event undergone by the commercial base esters and gives rise to 52.5-67.3 % mass loss. It occurs in a similar temperature range (236-254 ^{o}C) to event 2 observed for the triglycerides and therefore represents a combination of ester evaporation and oxidation. The highly unsaturated ester B loses less mass over event 2 than the more saturated A and C esters as a result of its greater susceptibility to residue-forming reactions such as polymerisation. The high levels of unsaturation within ester B also produce two discernable mass loss peaks within event 2, with the peak at lower temperature (~ 230 ^{o}C) resulting from the formation and decomposition of hydroperoxides.[5, 6, 17, 18]

The final mass loss event within the primary decomposition region is event 3, which occurs in the range 267-286 ^{o}C. Ester B loses almost twice as much mass over this event (16.6 %) as esters A or C, indicating that event 3 is due to the secondary oxidation and/or recombination reactions of radicals following the complete consumption of C=C bonds via radical addition.[6, 18]

Table 3.6 Summary of TGA thermo-oxidative decomposition data for the seven triglycerides. Errors are less than ± 5 % except for the % residue at 500 ^{o}C (± 20 %).

Ester	T_{onset} (^{o}C)	T_{max} Event 1 (^{o}C)	Mass Loss Event 1 (%)	T_{max} Event 2 (^{o}C)	Mass Loss Event 2 (%)	T_{max} Event 3 (^{o}C)	Mass Loss Event 3 (%)	T_{max} Event 4 (^{o}C)	Mass Loss Event 4 (%)	T_{max} Event 5 (^{o}C)	Mass Loss Event 5 (%)	% Residue at 500 ^{o}C
A	216	175	5.46	250	67.3	275	9.28	314	10.5	473	4.48	0.36
B	211	173	3.38	257 *	52.5	286	16.6	323	15.3	481	9.42	2.8
C	199	197	25.2	236	60.3	267	8.95	310	5.23	464	1.88	0
Coconut Oil	231	-	-	256	76.7	-	-	323	15.2	477	5.89	1.7

* Event 2 for sample B contains two overlapping decomposition events, however the proportions of these events vary between runs.

Event 4 is the first mass loss event to occur within the secondary decomposition region and appears at 310-323 ^{o}C. Given that event 4 is observed at approximately the same temperature for both the triglycerides and the commercial base esters, it indicates the removal of high molecular weight material via thermal decomposition reactions such as cracking and decarboxylation.[23, 24, 48] Despite its high levels of alkyl chain unsaturation, ester B loses a similar amount of mass to coconut oil over event 4 (15.3 %), whereas the semi-synthetic derivatives undergo only 10.5 % (ester A) and 5.23 % (ester C) mass loss. These low levels of high temperature mass loss imply that the commercial esters volatilise more effectively at lower temperatures and are more resistant to the crosslinking reactions that form thermally stable products. The particularly low level of event 4 mass loss and lower peak temperature observed for ester C suggests that the crosslink density of the high molecular weight residues formed is considerably less than for tri-esters of the same alkyl chain composition.

The final mass loss event (event 5) represents the thermal decomposition and/or volatilisation of persistent radical recombination and soap-like residues.[4] Event 5 occurs at lower temperature and results in significantly less mass loss in ester C than in coconut oil or its semi-synthetic tri-ester derivative, ester A. In comparison to tri-esters of similar alkyl chain composition and more highly unsaturated esters, the di-ester possesses both greater volatility and a lower concentration of radical species available to undergo recombination. These factors limit the availability of reactants to form metal-carboxylates and radical recombination products at higher temperatures, resulting in residue that is both less thermally stable and present in lower amounts.

The highly unsaturated ester B loses approximately twice as much mass over event 5 as the more saturated ester A and the material decomposed is more thermally stable, with the peak mass loss temperature for ester B being ~ 8 ^{o}C above that of ester A. Despite this, ester B leaves significantly less residue (2.8 %) at 500 ^{o}C than comparably unsaturated triglycerides. Esters A and C leave 0.36 % and 0 % residue at 500 ^{o}C respectively.

3.2.3.2 Thermo-Oxidative Decomposition Profile by PDSC

The PDSC results obtained for coconut, palm and cottonseed oils are representative of those obtained for the other triglycerides and for the three commercial base esters and figure 3.12 shows an overlay of the heat flow vs temperature plots for these samples. A summary of the onset points (T_{onset}), exotherm and endotherm temperatures (T_{max}) and respective enthalpies for all ester samples is provided in table 3.7.

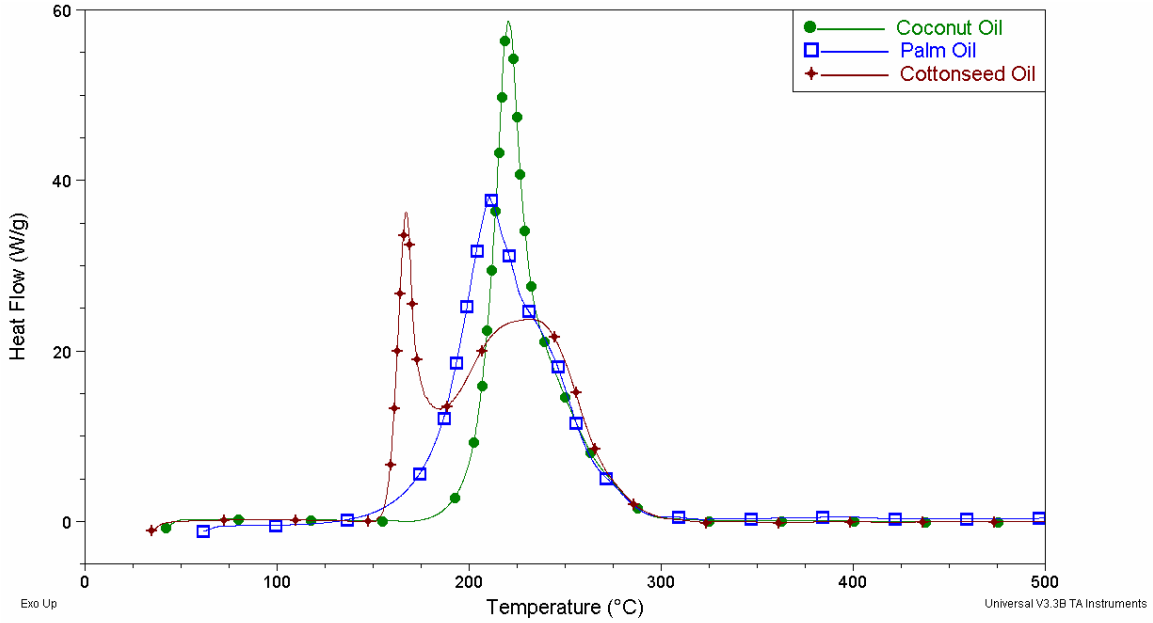

Figure 3.12 Overlay of the PDSC thermograms of coconut, palm and cottonseed oils.

The primary decomposition region for the triglycerides and commercial base esters is highly complex; the majority of esters show three distinguishable exotherms, however as many as five exotherms may be superimposed upon one another. The enthalpies associated with these exotherms increase with increasing levels of unsaturation and esters containing high levels of polyunsaturates display enthalpies that are proportionately greater than those measured for esters high in monounsaturates. In agreement with the findings made by TGA, these factors imply that the events observed

for the triglycerides and base esters within the primary decomposition region are associated with oxidation reactions including hydroperoxide formation, the formation radical species and the subsequent polymerisation, secondary oxidation and recombination reactions of these species.[19, 20, 49]

The first event observed in the ester PDSC profiles is exotherm 1, a sharp exotherm for which the peak temperature and enthalpy varies widely and can be used to broadly categorise the esters into three groups. The first group, comprising of coconut oil and the two semi-synthetic base esters, displays exotherm 1 peak temperatures in the range 216-220 ^{o}C and enthalpies that contribute to 62.0-64.6 % of the total heat flow. The low levels of alkyl chain unsaturation in these esters impart a strong resistance to oxidation so that processes such as hydroperoxide formation and decomposition do not contribute to a significant proportion of heat flow. Instead, as observed for methyl stearate in 3.1, thermal cracking and combustion-type reactions are the dominant exothermic processes.[7, 8, 23, 48] This is evidenced by the sharp profile of exotherm 1 as well as peak maximum heat flows that are up to 50 % greater than those observed for the other esters.

The second group of esters (cottonseed, sesame, canola and safflower oils) contain high levels of mono- and/or polyunsaturated alkyl chains culminating in a lower resistance to oxidation. Hydroperoxide formation and decomposition are therefore the dominant processes contributing to heat flow, as indicated by exotherm 1 occurring at much lower peak temperatures in these esters (148-169 ^{o}C) and contributing to a mere 23.5-27.0 % of the total heat flow.[50] The thermal cracking and combustion reactions observed in esters containing predominantly saturated alkyl chains are unfavourable at these lower temperatures.[8, 24]

The third group of esters (palm oil and commercial base ester B) display exotherm 1 characteristics that reflect their intermediate resistance to thermo-oxidative decomposition. The exotherm 1 peak temperatures associated with these esters are 211 ^{o}C and 213 ^{o}C respectively, and suggest an oxidative stability similar to that observed for coconut oil and its derivatives.

Table 3.7 Summary of PDSC data for the triglycerides and commercial base esters. Errors are less than ± 10 % for all temperature measurements and for all primary region enthalpy measurements.

Triglyceride/ Ester	T_{onset} (^oC)	Primary Region Room Temperature-300 ^oC						Secondary Region > 300 ^oC					
		Exotherm 1		Exotherm 2		Exotherm 3		Exotherm 4		Endotherm 1		Total Region	
		T_{max} (^oC)	ΔH (J g^{-1})	T_{max} (^oC)	ΔH (J g^{-1})	T_{max} (^oC)	ΔH (J g^{-1})	T_{max} (^oC)	ΔH (J g^{-1})	T_{max} (^oC)	ΔH (J g^{-1})	T_{max} (^oC)	ΔH (J g^{-1})
Coconut Oil	206	220	6840	242	3330	274	614	306	51.4	322	2.56	369	136
Palm Oil	181	211	7870	240	3490	275	715	309	62.2	324	4.38	393	178
Cottonseed Oil	156	165	2970	226	8830	276	660	306	49.7	322	2.97	396	175
Sesame Oil	158	169	3420	228	9900	277	664	307	80.0	324	2.50	389	248
Canola Oil	146	162*	3580	216*	9740	279	763	309	115	325	8.06	407	340
Safflower Oil	136	148	5710	241	13910	276	1139	330	107	354	3.66	401	368
Castor Oil	191	201#	6450	239	4740	-	-	307	43.8	319	4.67	376	245
Ester A	200	218	6690	246	3540	-	-	307	48.8	324	1.90	396	166
Ester B	171	213	9380	248	3820	-	-	310	171	332	7.32	411	553
Ester C	200	216	6810	244	3200	276	309	303	59.9	324	2.03	341	219

* Additional peaks at ~ 172 ^{o}C and 233 ^{o}C are visible within exotherms 1 and 2 respectively for canola oil.
# Exotherm 1 for castor oil comprises of two overlapping exotherms at 201 ^{o}C and 207 ^{o}C.

Exotherm 1 constitutes approximately 66 % of the total heat flow for these esters, inferring that it does not solely comprise of oxidative processes such as the formation and decomposition of hydroperoxides. Although the peak maximum heat flows measured for palm oil and ester B are ~ 35 % lower than for coconut oil, it is likely that both oxidation and thermal cracking reactions contribute to exotherm 1.

As observed by TGA, the oxidative decomposition profile of castor oil measured by PDSC is unique; exotherm 1 occurs at much higher peak temperature (~ 201 ^{o}C) than in other highly unsaturated triglycerides. The sharpness of this exotherm, together with its high maximum heat flow and significant enthalpy (~ 56 % of the total heat flow) suggest that it is dominated by thermal cracking and combustion processes. However, unlike coconut oil and its derivatives, an additional peak is superimposed upon exotherm 1 in castor oil, giving rise to a 'shoulder' at ~ 207 ^{o}C. This shoulder represents the condensation polymerisation of hydroxyl groups contained in ricinoleic acid moieties via scheme 3.6 above.

The second exotherm within the primary decomposition region (exotherm 2) occurs in the temperature range 216-248 ^{o}C. It is a broad peak consisting of multiple overlapping processes that are resolved in the PDSC profiles of triglycerides such as canola oil. Exotherm 2 occurs at higher peak temperature in triglycerides such as cottonseed and safflower oil, which contain proportionately greater amounts of polyunsaturated alkyl chains. This observation is consistent with the nature of the reactions that are represented by exotherm 2, including the polymerisation, secondary oxidation and recombination reactions of radical species formed during exotherm 1.[7, 8, 50] As discussed above with respect to TGA, due to the low initial concentrations of radical species within the triglyceride and base ester samples, radical addition to C=C bonds in the ester alkyl chains occurs preferentially to radical decomposition or recombination.[6] Therefore, the low-temperature end of exotherm 2 represents the formation of high molecular weight and crosslinked deposits via radical addition reactions. Following the complete consumption of C=C bonds, radical species then undergo the more favourable secondary oxidation reactions, followed by radical recombination.

The higher exotherm 2 peak temperatures measured for polyunsaturated triglycerides result from higher final concentrations of radical species giving rise to a greater contribution from radical decomposition and recombination reactions. The exotherm 2 enthalpies of reaction measured for the triglyceride samples reflect these observations and follow the same trend as for exotherm 1, with the exception of castor oil; the exotherm 2 enthalpy measured for castor oil is considerably lower (~ 4740 J g^{-1}) than the enthalpies measured for other highly unsaturated triglycerides due to limited radical formation (shown by scheme 3.6).

As observed for methyl esters, the triglyceride and base ester secondary decomposition region (300-500 ^{o}C) appears as a tail-like transition consisting of a series of overlapping endotherms and exotherms. These represent reactions including the formation of metal carboxylate complexes and the thermal cracking and combustion of residual hydrocarbons. The first secondary decomposition region feature observed for both the triglycerides and the commercial base esters is a small exotherm (exotherm 4 in table 3.7) that occurs in the range 303-330 ^{o}C. Exotherm 4 partially overlaps with events in the primary decomposition region and both its enthalpy and peak maximum temperature generally increase with increasing levels of ester unsaturation. Despite this, and in contrast to the oxidation reactions observed during the primary decomposition region, there is no distinctive relationship between the proportions of mono- and polyunsaturated alkyl chains in the esters and the magnitude of exotherm 4 or the temperature at which it occurs; highly polyunsaturated triglycerides such as cottonseed and safflower oil do not display exotherm 4 peak temperatures or enthalpies that are proportionately higher/lower than the corresponding values measured for triglycerides containing high levels of monounsaturates. This suggests that exotherm 4 is dependent upon the amount of thermally stable material present and it is not associated with the extent of crosslinking within this material. Exotherm 4 is therefore likely to represent the formation of metal carboxylate complexes, or ‘soaps’, according to scheme 3.4.

The most notable feature in the ester secondary decomposition profiles is an endotherm that occurs immediately after exotherm 4 in the range 319-353 ^{o}C. This endotherm is

present in the thermograms of all triglycerides and commercial base esters and corresponds to the initiation of thermal cracking reactions.[7, 8] It is shifted to higher temperatures and increases in enthalpy in more highly unsaturated - and polyunsaturated – triglycerides, representing the greater thermal stability of more densely crosslinked deposits and the larger amounts of energy required to decompose them. Castor oil is an exception to this as a result of the different chemical nature of its polymerised residues, and its decomposition initiation endotherm occurs at 319 ^{o}C, a temperature below that of coconut oil. Despite this, the total enthalpy and maximum peak temperature value measured over the secondary decomposition region for castor oil are similar to those of canola and safflower oils, indicating that a considerable amount of high molecular weight material is decomposed over this region.

The trend in decomposition initiation for the other triglycerides is mimicked in the total secondary decomposition region enthalpy and maximum peak temperature values obtained. These decomposition reactions are not complete at 500 ^{o}C and exothermic events for sesame, canola and safflower oils in particular are commencing at > 460 ^{o}C temperatures. This is in agreement with observations made by TGA, whereby as much as 7 % residue remains at 500 ^{o}C.

Figure 3.13 shows a comparison between TGA and PDSC onset point results for the triglycerides and commercial base esters. The trend in triglyceride oxidation onset temperature by PDSC mirrors that obtained by TGA. The onset points of the triglycerides decrease with increasing levels of alkyl chain unsaturation and triglycerides high in polyunsaturated fatty acid chains are proportionately less stable towards oxidation than those high in monounsaturates; safflower oil gives a onset point value 10 ^{o}C below that of canola oil despite the fact that canola oil contains a greater total percentage of unsaturated alkyl chains. Similarly, the PDSC onset points for semi-synthetic esters A and C are close to that of coconut oil whilst the onset point of the fully-synthetic ester B is lower as a result of its 100 % oleate alkyl chain composition. The high oxidative stability of castor oil given its considerable levels of unsaturation is in agreement with results obtained by TGA and the findings of others.[46]

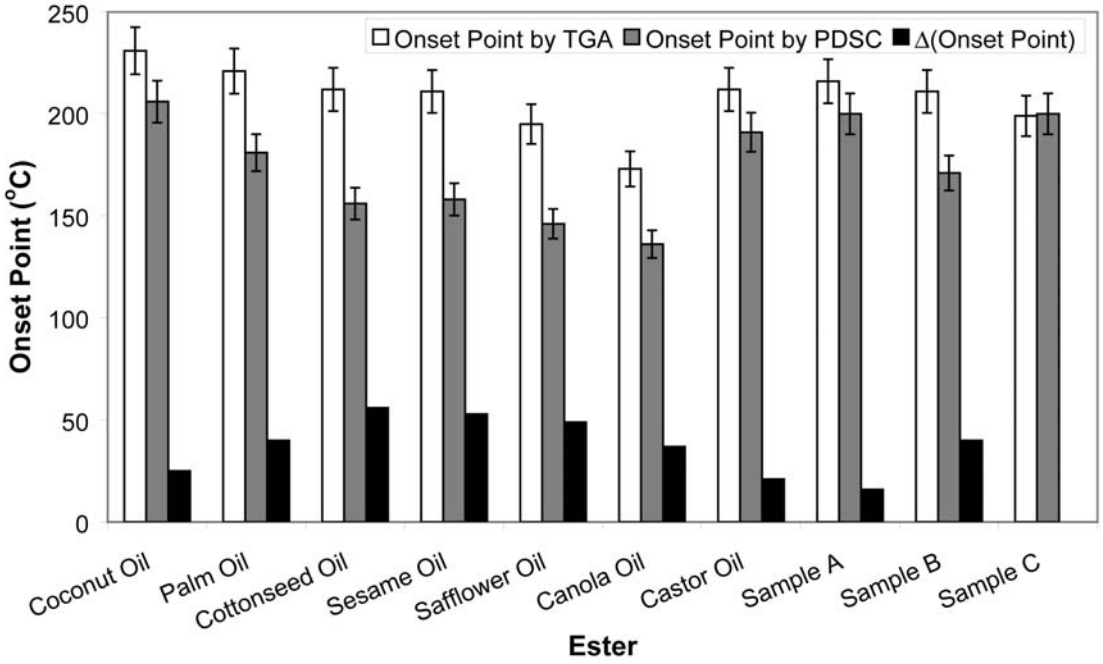

Figure 3.13 Comparison between the onset temperatures of mass loss (TGA) and oxidation (PDSC) for the triglycerides and commercial base esters. The error margin is less than ± 5 %.

The difference between the TGA and PDSC onset points, Δonset point, is indicative of the reactivity of an ester towards oxidative polymerisation; esters with large Δonset point values undergo exothermic reactions at low temperature that do not lead to the evolution of volatile material. Figure 3.13 shows that Δonset point increases with increasing alkyl chain unsaturation levels and is greater in esters containing large amounts of polyunsaturates. This is in accordance with the findings in section 3.1 and confirms that highly unsaturated esters undergo polymerisation reactions at low temperatures do not generate volatile products. The strong resistance of the commercial base esters to polymerisation is emphasised by the low Δonset point values of these samples in comparison to triglycerides containing similar unsaturation levels.[10, 35]

3.2.3.3 Thermo-Reductive Decomposition Profile by TGA

TGA analysis of four representative triglycerides, coconut, sesame, safflower and castor

oils, and the three commercial base esters gives the thermo-reductive decomposition profiles shown in figures 3.14A and 3.14B respectively. Table 3.8 presents a summary of the onset points (T_{onset}), peak temperatures (T_{max}) and relevant mass losses.

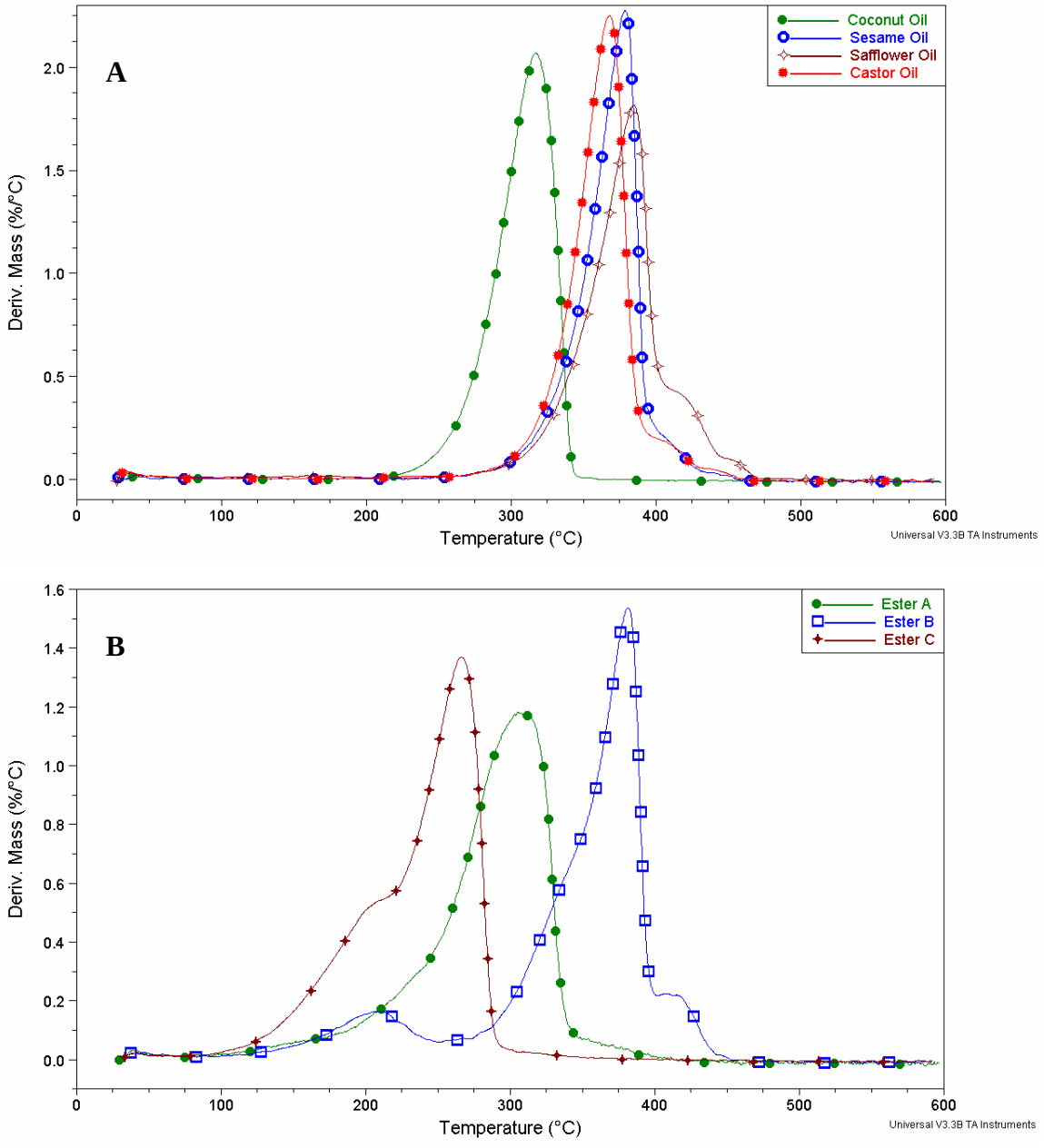

Figure 3.14 Overlay of the TGA thermo-reductive decomposition profiles (DTG curves) of four representative triglycerides (A) and the commercial base esters (B).

Table 3.8 Summary of TGA thermo-reductive decomposition data for the triglycerides and commercial base esters. Errors are less than ± 10 % except for the % residue at 500 °C (± 20 %).

Ester	T_{onset} (°C)	T_{max} Event 1 (°C)	Mass Loss Event 1 (%)	T_{max} Event 2 (°C)	Mass Loss Event 2 (%)	T_{max} Event 3 (°C)	Mass Loss Event 3 (%)	T_{max} Event 4 (°C)	Mass Loss Event 4 (%)	% Residue at 500 °C
Coconut Oil	277	-	-	317	97.0	-	-	-	-	1.5
Palm Oil	322	-	-	367	85.4	395	8.12	433	1.10	1.9
Cottonseed Oil	328	-	-	373	88.3	405	7.22	440	0.802	2.1
Sesame Oil	334	-	-	379	90.7	410	5.48	440	0.539	2.4
Canola Oil	330	-	-	376	83.5	408	11.0	440	1.63	2.5
Safflower Oil	339	-	-	384	85.9	415	12.6	453	1.64	1.2
Castor Oil	327	-	-	367	92.7	408	4.74	441	0.635	1.2
Ester A	250	-	-	244	18.4	310	74.9	359	2.47	0
Ester B	164*	206	12.6	342	30.4	380	48.4	408	6.35	2.7
Ester C	201	-	-	211	32.9	265	64.4	306	1.17	0

* The T_{onset} value for ester B's largest mass loss event (event 2) is 312 °C.

The thermo-reductive decomposition profiles of the triglycerides and commercial base esters are remarkably different to those obtained under oxygen. The triglyceride onset temperatures of mass loss under HNX range from 277 ^{o}C (coconut oil) up to 339 ^{o}C (safflower oil), values which are 50-160 ^{o}C higher than the corresponding T_{onset} values measured under oxygen. Similarly, the peak maximum temperature for the first of the three mass loss events observed for the triglycerides (event 2; ester B is the only sample to display mass loss over event 1, as will be discussed below) occurs in the range 317–384 ^{o}C (T_{max} for the first mass loss event observed under oxygen ranges between 183-228 ^{o}C), indicating that the triglycerides are considerably more stable under HNX.

Although a comparable trend is observed for the commercial base esters, the increase in stability afforded by the use of HNX is less marked. For example, the thermo-reductive T_{onset} and event 2 T_{max} values measured for ester C (T_{onset} = 201 ^{o}C; T_{max} = 211 ^{o}C) are only 2 ^{o}C and 14 ^{o}C higher than the corresponding values measured under oxygen (T_{onset} = 199 ^{o}C; T_{max} = 197 ^{o}C). Whilst ester B's event 1 peak maximum temperature under HNX (206 ^{o}C) is greater than that under oxygen (173 ^{o}C), its HNX T_{onset} value is lower. This anomaly, together with the above observations, can be rationalised by considering the processes which give rise to ester mass loss under HNX.

In the presence of oxygen, the ester thermal decomposition process is governed by oxidative stability; highly unsaturated esters possess poor resistance to oxidation and undergo mass loss at lower temperatures than do esters containing predominantly saturated alkyl chains.[3] In contrast, an HNX atmosphere precludes oxidative decomposition reactions from occurring such that T_{onset} and T_{max} are independent of oxidative stability. Instead, ester mass loss is proportional to volatility, which is primarily determined by molecular weight.[3, 10, 51] This is confirmed by the results in table 3.8 as safflower oil, a highly unsaturated triglyceride, displays T_{onset} and T_{max} values that are greater than those of comparatively saturated triglycerides such as coconut oil. Figure 3.15 shows a plot of the T_{onset} and event 2 T_{max} values measured for the triglycerides as a function of average triglyceride molecular weight.

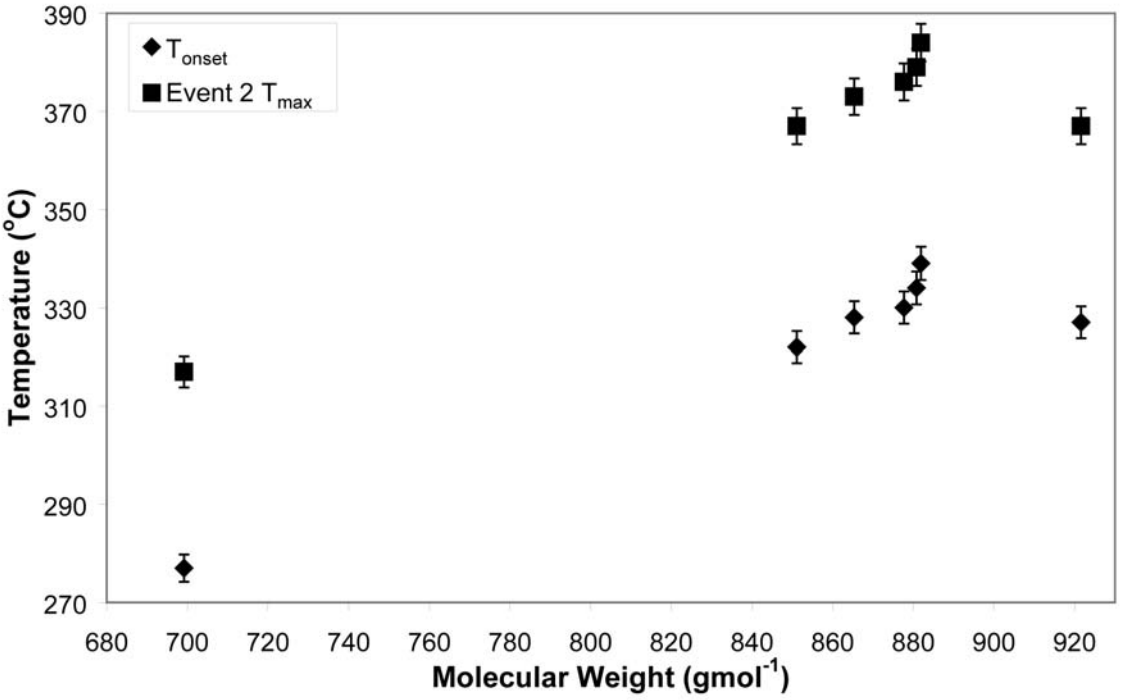

Figure 3.15 T_{onset} and event 2 T_{max} values (obtained from TGA thermo-reductive decomposition data) as a function of average triglyceride molecular weight. The error bars represent ± 1 % error.

T_{onset} and event 2 T_{max} increase with increasing triglyceride molecular weight for all triglycerides except castor oil. Coconut oil, which comprises ~ 50 % by mass of laurate alkyl chains (C12:0), has a considerably lower average molecular weight (699 g mol^{-1}) than the other triglycerides and displays the lowest T_{onset} and event 2 T_{max} values (277 ^{o}C and 317 ^{o}C respectively). The increase in T_{onset} and T_{max} observed for triglycerides of higher molecular weight is independent of the presence of unsaturated alkyl chains; sesame oil and safflower oil are of similar molecular weight (881 g mol^{-1} and 882 g mol^{-1} respectively) but safflower oil contains far more polyunsaturated alkyl chains and yet the T_{onset} and event 2 T_{max} values measured for the two triglycerides are within experimental error margins. Although these observations contradict the findings of Sathivel et al.,[3] who determined that increasing the number of C=C bonds in a fatty acid alkyl chain increases the proportion of fatty acid mass lost at lower temperatures under a

nitrogen atmosphere, they confirm that the low-temperature triglyceride mass loss process results from evaporation as opposed to thermal decomposition. An anomalous result is obtained for castor oil, which possesses the highest average molecular weight (922 $gmol^{-1}$) but displays T_{onset} (327 ^{o}C) and event 2 T_{max} (367 ^{o}C) values which are lower than those measured for the majority of the other triglycerides. This is likely to be due to the presence of the OH functionality, whose condensation reactions do not rely on the availability of oxygen (scheme 3.6).

The different T_{onset} and T_{max} trend observed for the commercial base esters is due to the presence of free fatty acids and mono-/di-esters, which evaporate at low temperatures due to their lower molecular weights.[33] A discrete mass loss event (event 1) representing the volatilisation of free fatty acids is observed in the DTG profile of ester B whilst event 2, which occurs over the temperature range 211-342 ^{o}C and gives rise to 18.4-32.9 % mass loss, corresponds to the evaporation of mono-/di-esters. Event 2 observed for esters A and C is likely to include the volatilisation of both free fatty acid and mono-/di-ester components.. Event 3 (T_{max} = 265-380 ^{o}C) accounts for the majority of the base ester mass loss (48.4-74.9 %) such that it indicates tri-ester evaporation. Finally, event 4 (T_{max} = 306-408 ^{o}C) occurs within the reported temperature range over which thermal cracking and ester decarboxylation occur[23, 24] such that the small proportion of mass loss (1.17-6.35 %) represented by this event indicates the evolution of volatile short-chain hydrocarbons (such as CH_4), carboxylic acids and alcohols according to schemes 1.17-1.18 in Chapter 1.

Similarly, event 2 observed for the triglycerides accounts for the majority of sample mass loss (83.5-97.0 %) and corresponds to triglyceride molecule evaporation. Event 3 (T_{max} = 395-415 ^{o}C; 4.74-12.6 % mass loss) observed for all the triglycerides except coconut oil signifies the occurrence of decarboxylation/thermal cracking reactions. Such reactions are absent in the coconut oil thermo-reductive decomposition profile due to coconut oil's low molecular weight and complete volatilisation at lower temperatures. Finally, event 4 occurs at similar temperature to events 4 and 5 observed under thermo-oxidative conditions (T_{max} = 433-453 ^{o}C) and therefore represents further thermal

cracking reactions and the decomposition of any carboxylate residues formed at lower temperatures due to reactions between the triglycerides and the aluminium pan surface. The fact that event 4 under HNX accounts for considerably less sample mass loss (0.635-1.64 %) than under oxygen (5.89-18.1 %) is due to the facilitation of triglyceride evaporation at lower temperatures.

Accordingly, the triglyceride and base ester decomposition process is complete at temperatures below 500 ^{o}C and considerably less residue is present at 500 ^{o}C; triglyceride residues range between 1.2-2.5 % as opposed to 1.7-7.9 % (under oxygen).

3.2.3.4 Analysis of Hydrogenated Triglyceride Derivatives

Hydrogenation was used to create saturated analogues of two triglycerides, cottonseed and sesame oil. Reaction progress was monitored by ^{1}H NMR and the spectra obtained for non-hydrogenated and hydrogenated sesame oil are presented in figure 3.16.

A decrease in the intensity of the triplet signal at 2.77 ppm (-CH=CH-C**H$_2$**-CH=CH-) and two multiplets at 2.00-2.06 ppm (-C**H$_2$**-CH=CH-) and 5.30-5.37 ppm (-C**H**=C**H**-) confirms the consumption of C=C bonds.[52] The ^{1}H NMR spectra of the hydrogenated sesame and cottonseed oil products indicate that a large reduction in C=C bond concentration was achieved. A comparison between the normalised peak areas of the three characteristic C=C bond signals in the hydrogenated products and the corresponding normalised peak areas for the untreated triglyceride samples (the area of the -C**H$_2$**- multiplet at 1.57-1.63 ppm was used as the normalisation factor) shows that 80 % and 90 % of C=C bonds were successfully hydrogenated in cottonseed and sesame oils respectively.

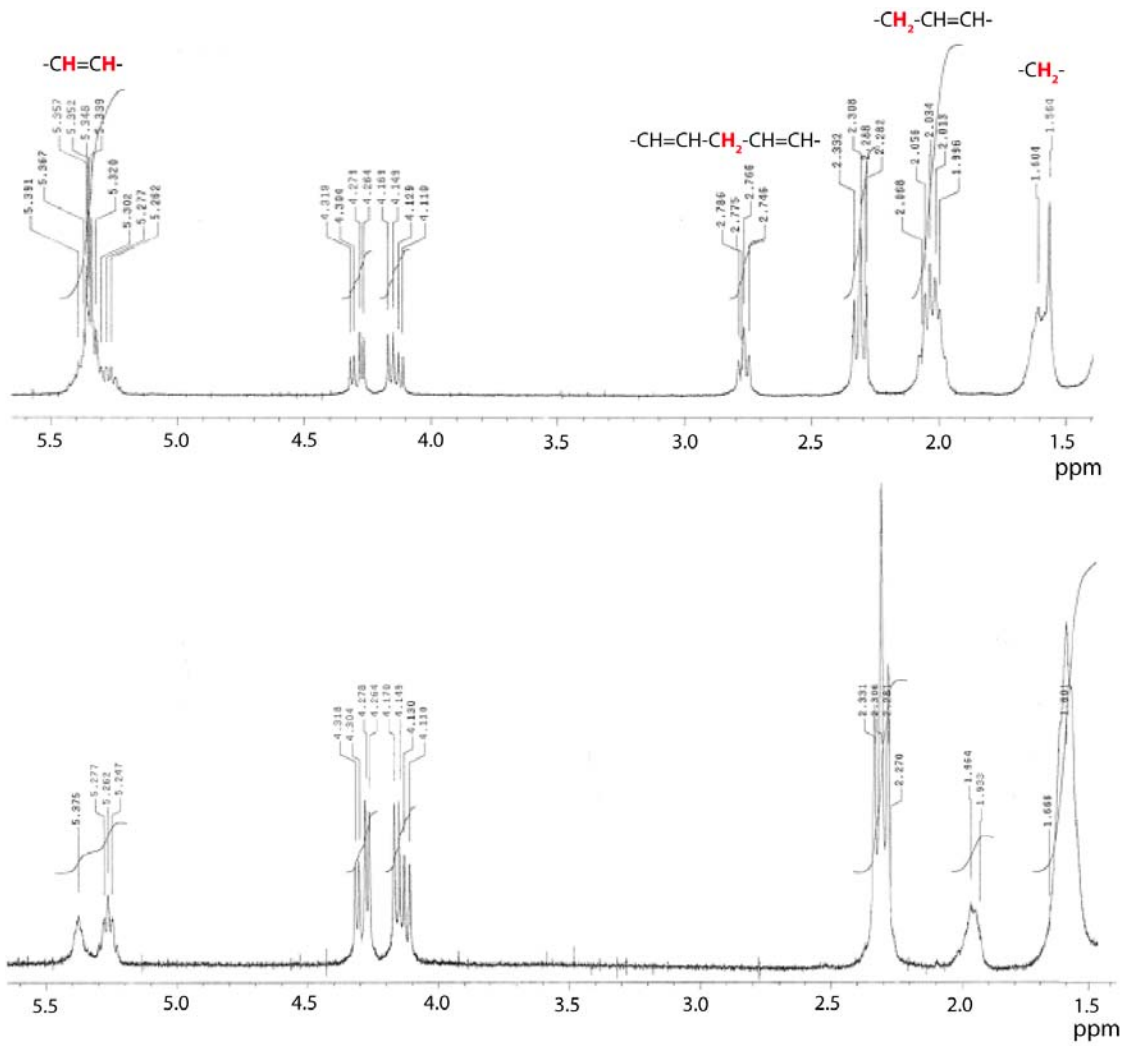

Figure 3.16 ^{1}H NMR spectra of sesame oil and hydrogenated sesame oil.

Figures 3.17A and 3.17B compare the TGA and PDSC thermo-oxidative decomposition results for hydrogenated and non-hydrogenated sesame oil. These results are representative of those obtained for the corresponding cottonseed oil samples. Decreasing the C=C bond concentration induces several notable changes to sesame oil's thermo-oxidative decomposition profile. The TGA results for the hydrogenated sesame oil product show that no mass increase corresponding to oxygen uptake is observed prior to the onset of mass loss, confirming an increased resistance to oxidation as a result of

lower alkyl chain unsaturation levels. Event 1, which typically occurs at 215 ^{o}C in untreated sesame oil and results from the formation and decomposition of hydroperoxide species, is absent in the TGA thermogram of hydrogenated sesame oil, further demonstrating an increased oxidative stability.

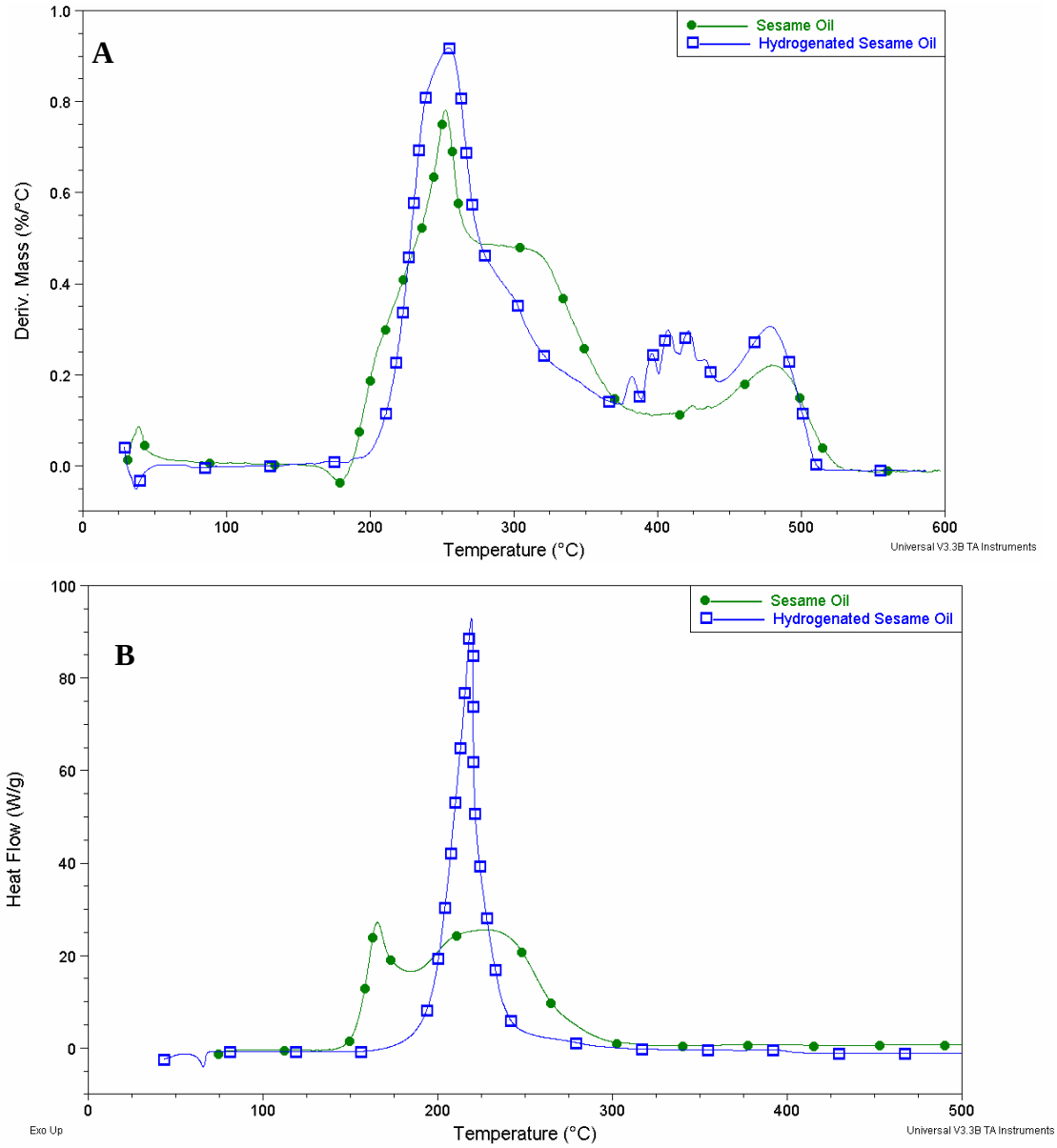

Figure 3.17 Overlay of the TGA (A) and PDSC (B) thermo-oxidative decomposition profiles of hydrogenated and non-hydrogenated sesame oil.

In contrast, the proportion of mass lost over event 2 is considerably higher in the hydrogenated sample (45.0 % as opposed to 27.4 % in untreated sesame oil). A similar proportion of mass loss is observed during event 2 in highly saturated triglycerides such as palm oil and is primarily ascribed to evaporation. Analogous observations are made with respect to event 3 such that oxidation processes are minimised by the removal of C=C bonds (although in accordance with the NMR results shown above, a small proportion of C=C bonds remain in the hydrogenated sesame oil sample such that oxidation is not entirely precluded).

A series of up to five sharp mass loss peaks are observed between 395–432 ^{o}C for the hydrogenated sesame oil, giving rise to a total mass loss of ~ 13.0 %. Analogous peaks are present in the DTG curves of untreated sesame, cottonseed and canola oils and are attributable to thermal cracking reactions. The prominence of these peaks in hydrogenated sesame oil is due to the presence of large amounts of non-oxidised triglyceride material containing long, saturated alkyl chains.

Finally, the mass loss observed for the hydrogenated sesame oil sample during event 5 occurs at similar temperature to the untreated oil (T_{max} for both samples = 479 ^{o}C), however it accounts for a slightly smaller proportion of the total mass loss (12.3 % as opposed to 10.8 %). This indicates that less thermally stable residue is formed by decomposition of the hydrogenated sesame oil. Furthermore, the hydrogenated sesame oil decomposition end temperature is shifted by ~ 19 ^{o}C to 516 ^{o}C (T_{end} for the untreated oil = 535 ^{o}C), reducing the amount of residue left at 500 ^{o}C to 2.9 %.

The PDSC profile obtained for the hydrogenated sesame oil is similar to that of coconut oil, the most highly saturated triglyceride studied. The increased resistance to oxidation observed by TGA is corroborated by the significantly higher PDSC oxidation onset temperature measured for the hydrogenated sample (T_{onset} = 198 ^{o}C; T_{onset} for untreated sesame oil = 158 ^{o}C). The fact that T_{onset} by PDSC is only 22 ^{o}C less than T_{onset} by TGA (220 ^{o}C), as opposed to 53 ^{o}C less for untreated sesame oil, also supports this observation.

Exotherm 1 is shifted to considerably higher temperature in the hydrogenated sample

(T_{max} = 219 ^{o}C as opposed to 169 ^{o}C in untreated sesame oil) and contributes to a far greater proportion of the total heat flow (~ 61 % as opposed to 24 %). This confirms a change in the reactions giving rise to sample decomposition from hydroperoxide formation/decomposition to combustion and thermal cracking.

Exotherm 2 (T_{max} = 226 ^{o}C) is barely apparent for the hydrogenated sample and corresponds to a mere 28 % of the total heat flow (cf 71 % for untreated sesame oil), evidencing a reduction in amount of radicals formed by oxidative decomposition during event 1 such that less polymerisation, secondary oxidation and radical recombination occurs. Accordingly, the secondary decomposition region accounts for only 1 % of the total heat flow, in good agreement with the lower residue measured by TGA.

These observations therefore confirm the identity of mass loss and heat flow events detected in untreated triglyceride samples and that the formation of large amounts of thermally-stable residue is directly related to high levels of alkyl chain unsaturation.

3.2.3.5 Evaluation of Residue Levels by the % B/A Ratio Technique

The residue-forming tendency of the esters can be determined by calculating the % B/A ratio according to equation 3.1.[7, 8] The triglycerides and base esters are considerably less volatile than methyl esters, shifting mass loss/heat flow events to higher temperature. Consequently, for the triglycerides and base esters, the primary region includes mass loss and heat flow events occurring between room temperature and 300 ^{o}C, whilst the secondary decomposition region includes events in the range 300-500 ^{o}C. A plot of the TGA and PDSC % B/A ratio results calculated for each of the triglycerides and commercial base esters is shown in figure 3.18.

As for the methyl esters studied in 3.1, the % B/A ratio values determined by PDSC are largely within the ± 10 % error limits associated with the measurement. This is due to the enthalpies of events in both the primary and secondary decomposition regions increasing with increasing alkyl chain unsaturation. However, a general trend towards increasing % B/A ratio with increasing triglyceride unsaturation levels is observed, suggesting that proportionately more energy is released by the thermal decomposition of

residues present above 300 ^{o}C in highly unsaturated triglycerides such as canola oil.

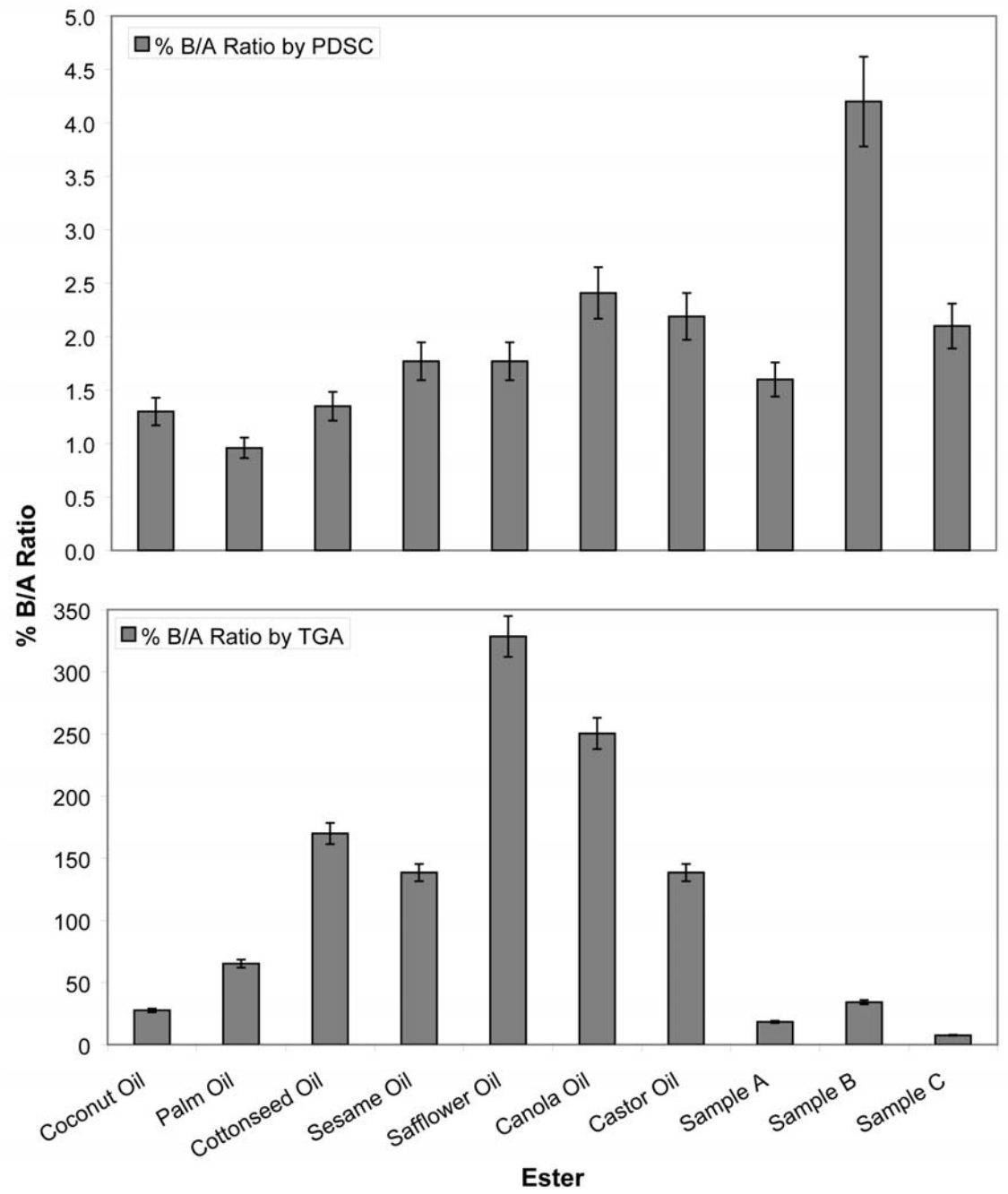

Figure 3.18 % B/A ratios determined for the triglycerides and commercial base esters by PDSC and TGA. The error bars represent ± 10 % and ± 5 % error for the PDSC and TGA results respectively.

This can result from the presence of greater amounts of residue and/or differences in residue chemical structure. Accordingly, the % B/A ratio values obtained for the two semi-synthetic base esters (esters A and C) are similar to that of coconut oil, whilst the unsaturated fully-synthetic ester B has a % B/A value of almost twice that of any other ester. Despite the general trend towards increasing % B/A ratio with increasing oil unsaturation, the PDSC % B/A ratio results do not distinguish between the proportion of mono- and polyunsaturated alkyl chains. However, the TGA results indicate that oils containing high polyunsaturation levels have a greater residue-forming tendency; cottonseed and safflower oils have higher TGA % B/A ratios than sesame and canola oils respectively. This confirms that changes in the PDSC % B/A ratio result from differing amounts of residue as opposed to variations in residue chemical structure.

The TGA % B/A ratio values obtained for semi-synthetic base esters A and C are significantly lower than for coconut oil, highlighting that the improved low-temperature volatility and resistance to oxidative polymerisation of these esters results in them leaving a lower amount of thermally stable residue than their naturally-occurring counterparts.[10, 35] As noted above, the chemical nature of the residues formed by the semi-synthetic esters is analogous to coconut oil; whilst the TGA results confirm that the semi-synthetic esters leave a lower amount of residue, no decrease in the enthalpy of residue decomposition is observed. In contrast, whilst the % B/A ratio by TGA for the fully-synthetic ester B is only marginally greater than that of coconut oil, its PDSC % B/A ratio is significant. This suggests that the chemical structure of the residue formed by ester B is different as a considerable amount of energy is evolved through the decomposition of a relatively small amount of residue. This anomaly is justified by considering the differences in the alkyl chain length distributions of the esters. The alkyl chains contained in ester B are all 18 carbon atoms long, whilst those contained in the other esters are, on average, much shorter. Given that the secondary region comprises mainly of thermal cracking and combustion-type reactions and that the enthalpy of combustion of an ester increases with increasing alkyl chain length,[51] the energy released by the decomposition of ester B residues is likely to be considerably greater

than for the other esters.

The % B/A ratio results confirm that highly unsaturated triglycerides, particularly those that contain large proportions of polyunsaturated alkyl chains, are more likely to have a detrimental effect on metallic coating quality. Semi-synthetic esters are to be preferred as they leave lower amounts of thermally stable residue.

3.2.3.6 ATR Characterisation of Thermo-Oxidative Decomposition Reactions

The thermo-oxidative decomposition chemistry of representative triglycerides (coconut oil, sesame oil, safflower oil and castor oil) and commercial base esters (esters A and B) was studied by ATR. The spectra obtained for sesame and castor oils at room temperature are representative of those acquired for the other esters and are shown in figure 3.19. Peak assignments for the room temperature spectra of all six esters are given in table 3.9.

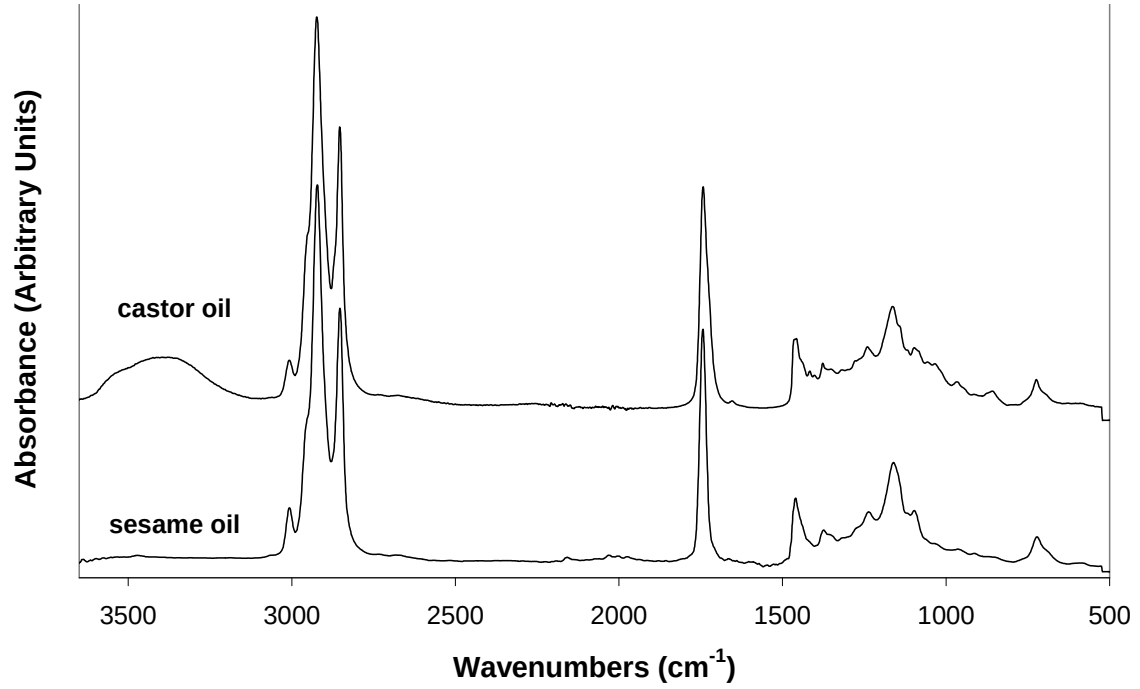

Figure 3.19 ATR spectra of sesame and castor oil acquired at room temperature.

Table 3.9 Peak assignments for the room temperature ATR spectra of coconut, sesame, safflower and castor oils and commercial base esters A and B.[27, 28]

Peak (cm^{-1})						Assignment
Coconut Oil	Sesame Oil	Safflower Oil	Castor Oil	Ester A	Ester B	
-	-	-	3379	3501	3528	νO-H (hydrogen-bonded)
-	3007	3008	3008	-	3003	νC-H (unsaturated)
2922	2922	2923	2924	2922	2922	νC-H in $–CH_2-$ (asymm.)
2853	2853	2853	2853	2853	2852	νC-H in $–CH_2-$ (symm.)
1743	1744	1743	1743	1740	1741	νC=O (esters)
1465	1460	1464	1458	1465	1463	γC-H in CH_2 / CH_3
-	-	-	1416	1418	1418	O-H bending
1377	1374	1377	1377	1380	1378	γ-CH_3 (symm.)
1230	1237	1238	1240	1234	1238	νC-O (esters)
1157	1161	1161	1163	1161	1159	
1111	1097	1099	1097	1113	1117	
963	964	967	967	967	967	γC-H in *trans* RCH=CH_2
722	722	723	724	722	722	CH_2 rocking; γC-H in *cis* C=C

ν = stretching; γ = out-of-plane deformation

asym. = asymmetrical; sym. = symmetrical

The sesame oil spectrum displays prominent bands at 3007 cm^{-1} (C-H stretching in unsaturated compounds), 1744 cm^{-1} (C=O stretching in esters), 1161 cm^{-1} (C-O stretch in esters) and 722 cm^{-1} (CH_2 rocking vibration). The room temperature spectra collected for coconut and safflower oil show similar features, however the unsaturated C-H stretching band in coconut oil is little more than a shoulder as a result of its low proportion of unsaturated alkyl chains. Castor oil contains analogous bands to the other

three triglycerides at 3008 cm^{-1}, 1743 cm^{-1}, 1163 cm^{-1} and 724 cm^{-1}, however additional bands are evident at 3379 cm^{-1} (O-H stretching) and 1416 cm^{-1} (O-H bending). These additional bands can be attributed to the presence of the hydroxyl functional group in ricinoleic acid alkyl chains and can be used to distinguish castor oil from the other triglycerides studied.

The spectrum of semi-synthetic ester A is similar to that of its parent triglyceride coconut oil, however the presence of free hydroxyl groups remaining on the polyfunctional alcohol as a result of incomplete trans-esterification is evidenced by O-H stretching and bending absorptions at 3501 cm^{-1} and 1418 cm^{-1} respectively. The O-H stretching absorption occurs at much higher wavenumber than in castor oil due to a lack of hydrogen bonding.[27] The presence of free fatty acids, as noted in the TGA results, is established by a shoulder on the ester C=O stretching band at lower wavenumber. The spectrum of fully-synthetic ester B is similar to that of ester A, however a band at 3003 cm^{-1} indicates high levels of unsaturation resulting from esterification with 100 % oleate fatty acids.

The bands at 3003-3008 cm^{-1} and 1740-1744 cm^{-1} can be monitored during the thermo-oxidative decomposition of the triglycerides and commercial base esters to identify changes to C=C bonds in the ester alkyl chain and the formation of radical recombination and secondary oxidation products. The O-H stretching region at ~ 3400 cm^{-1} can be monitored to detect the build up of hydroxyl-containing species such as hydroperoxides and acids in all ester samples. For castor oil, this region can also be used to observe polymerisation reactions undergone by the hydroxyl functional group on castor oil's ricinoleic acid alkyl chains (scheme 2).

Figures 3.20A and 3.20B show the ATR spectra obtained for thermo-oxidatively decomposed sesame and castor oils in the range 100-500 ^{o}C across the C=O (1870-1560 cm^{-1}, figure 3.20A) and O-H/C-H (3500-2780 cm^{-1}, figure 3.20B) stretching regions. The spectra acquired for coconut and safflower oils and the two commercial base esters are analogous to those of sesame oil. Table 3.10 provides a comparative summary of the thermo-oxidative decomposition steps undergone by all six ester samples.

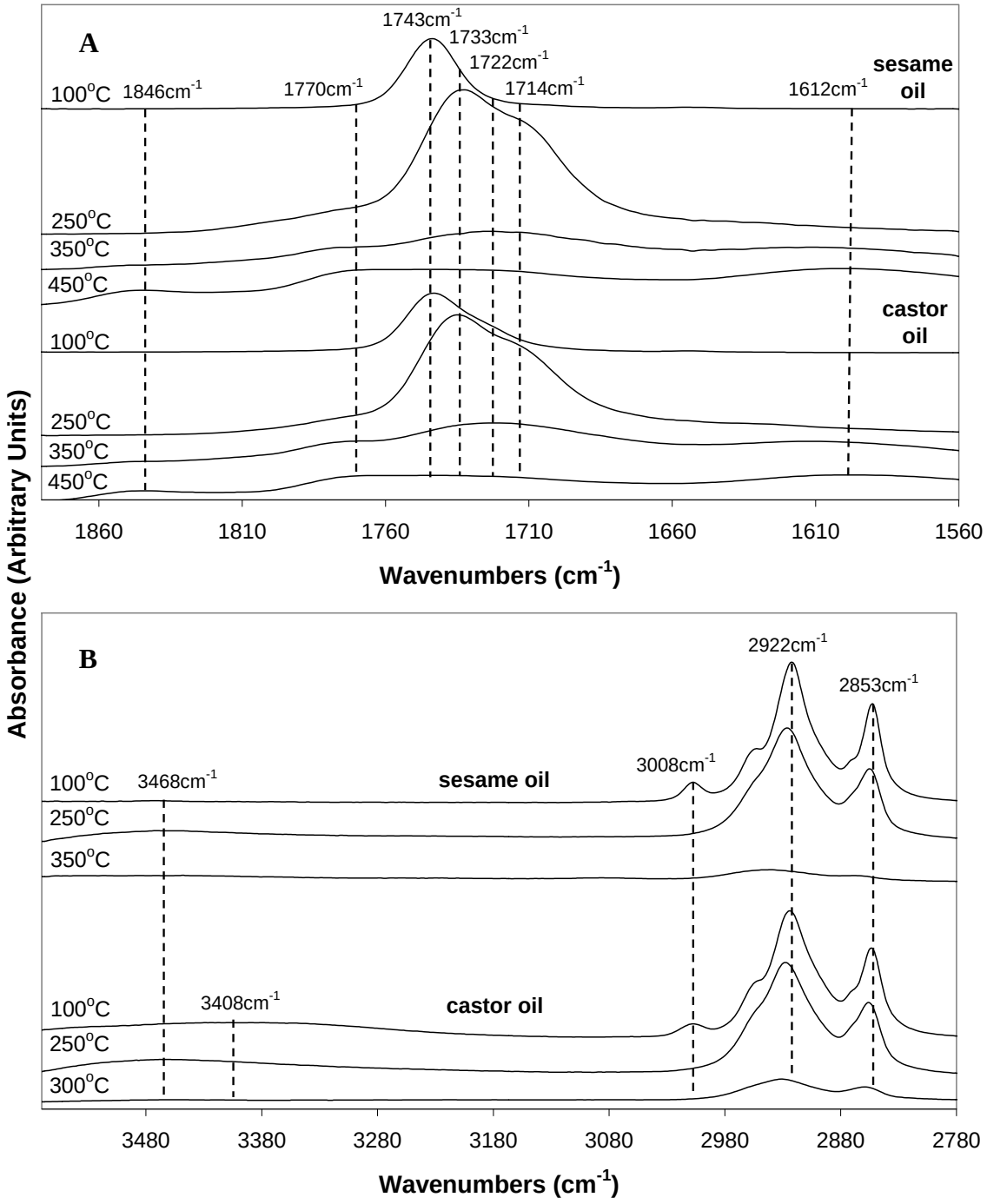

Figure 3.20 ATR spectra of thermo-oxidatively decomposed sesame and castor oil samples in the region 1870-1550 cm^{-1} (A) and 3500-2780 cm^{-1} (B).

Table 3.10 Summary of the temperatures at which spectral changes are observed for the triglycerides and commercial base esters. The observed changes are assigned to specific thermo-oxidative decomposition processes.

Spectral Change	Decomposition Process	Temperature Range (°C)					
		Coconut Oil	Sesame Oil	Safflower Oil	Castor Oil	Ester A	Ester B
Evolution of 3460 cm^{-1} band	Hydroperoxide formation	200-250	150-200	100-150	200-250	-	-
Disappearance of 3008 cm^{-1} band	Consumption of C=C; high molecular weight products	200-250	200-250	150-200	200-250	-	200-250
νC-H shifted to higher wavenumber	Ester breakdown; formation of volatile secondary oxidation products (acids, ketones, aldhehydes); initiation of radical recombination reactions (ethers, peroxides)	200-250	200-250	150-200	200-250	200-250	200-250
νC=O shifted to lower wavenumber		200-250	200-250	150-200	200-250	200-250	200-250
Evolution of 1733-1714 cm^{-1} bands		200-250	200-250	200-250	200-250	200-250	200-250
Evolution of 1770 cm^{-1} band		250-300	250-300	250-300	250-300	250-300	250-300
Disappearance of bands in νO-H region	Complete evaporation of volatile secondary oxidation products	250-300	300-350	250-300	250-300	250-300	300-350
Significant decrease in spectral intensity	Sample volatilisation/degradation	250-300	250-300	200-250	250-300	200-250	250-300
Evolution of 1612 cm^{-1} band	Formation of metal carboxylates	300-350	300-350	300-350	300-350	300-350	300-350
Evolution of 1847 cm^{-1} band	Recombination product build up	350-400	350-400	350-400	350-400	300-350	300-350
Disappearance of bands in νC-H region	Complete hydrocarbon chain decomposition	350-400	350-400	400-450	350-400	350-400	350-400
No spectral absorption	Complete residue decomposition	>500	>500	>500	>500	450-500	>500

For coconut, sesame and safflower oil, the thermo-oxidative decomposition process is initiated by the emergence of a broad O-H stretching band at ~ 3460 cm^{-1}, signalling hydroperoxide formation. The low temperature at which hydroperoxide formation occurs in safflower oil (100 ^{o}C) and the small amount of hydroperoxides formed in coconut oil (indicated by low O-H stretching intensity) verify that the triglyceride resistance to oxidative decomposition decreases with increasing unsaturation. In castor oil, a shift in the O-H stretching absorption from 3379 cm^{-1} to 3462 cm^{-1} is observed at 200 ^{o}C. As for the other triglycerides, this change indicates the commencement of oxidation. However, the comparatively high temperature at which the 3462cm^{-1} band is evolved, together with its high intensity and the complete disappearance of the 3379cm^{-1} band is in agreement with the simultaneous condensation of castor oil's ricinoleic acid O-H moieties to liberate water according to scheme 3.6. Hydroperoxide formation in the commercial base ester samples cannot be observed due to incomplete trans-esterification; free hydroxyl groups give rise to an O-H stretching absorption.

Following the initiation of the oxidation process, numerous spectral changes are observed in all the ester samples, including the disappearance of the unsaturated C-H stretching band at 3008 cm^{-1}, a shift in the C-H stretching absorptions at ~ 2922 cm^{-1} and 2853 cm^{-1} to higher wavenumber, broadening of the ester C=O stretching band and its shift to lower wavenumber and the evolution of a range of carbonyl species evidenced by the appearance of numerous bands in the range 1770-1714 cm^{-1}.

The first of these changes indicates the consumption of C=C bonds present in the triglyceride alkyl chains via radical addition and the subsequent formation of high molecular weight crosslinked deposits. The fact that these reactions occur at lower temperature in safflower oil (150 ^{o}C) than in the other three triglyceride samples (200 ^{o}C) testifies once more to the lower oxidative resistance of highly unsaturated triglycerides. In base ester A the consumption of C=C bonds cannot be observed due to the lower intensity of the unsaturated C-H stretching band. Despite ester B's high level of unsaturation, its C=C bonds are not consumed until 200 ^{o}C, confirming its greater resistance to oxidative polymerisation.

The shift in the C-H stretching absorptions to higher wavenumber, broadening of the C=O stretching band and evolution of multiple carbonyl stretching bands at lower wavenumber (1733 cm^{-1}, 1722 cm^{-1} and 1714 cm^{-1}) signify that the radical species formed by hydroperoxide decomposition have undergone side reactions, yielding secondary oxidation products such as alcohols, aldehydes, ketones and carboxylic acids. These changes are initiated at the same temperature for all the ester samples (~ 200 ^{o}C), however the temperature at which the volatilisation of the secondary oxidation products is complete varies. For ester A and coconut, safflower and castor oils, the intensity of the O-H stretching band is negligible after 250 ^{o}C. For ester B and sesame oil this band does not disappear until ~ 300 ^{o}C. These observations suggest that the occurrence of radical decomposition reactions in the ester A and coconut, safflower and castor oil samples is limited, or that the radicals and/or volatile secondary oxidation products formed are consumed by alternate reaction pathways. In coconut oil and ester A, limited hydroperoxide species are formed as a result of high saturation levels, whilst in castor oil, competing reaction pathways (scheme 3.6) interfere with the build up of secondary oxidation products, particularly carboxylic acids and alcohols. In safflower oil, the preferred reaction pathway of radicals is addition to C=C bonds, reducing the formation of secondary oxidation products. However in sesame oil and ester B, none of the above factors is dominant such that more secondary oxidation products are evolved and the volatilisation of these products is not complete until higher temperatures.

In all ester samples, the secondary oxidation product C=O stretching bands increase in intensity after the disappearance of the unsaturated C-H stretching band at ~ 3008 cm^{-1}, corroborating the findings of Oyman et al.[6] that the addition of radical species to C=C bonds (particularly in conjugated systems) takes place more readily than do radical decomposition or recombination reactions. In fact, radical recombination products are not observed until ~ 250 ^{o}C in all ester samples. At this temperature a broad band ~ 1770 cm^{-1} emerges, indicating the initial formation of peroxide, ether, lactone and cyclised carbonyl linkages.[11] These products continue to be evolved up until 300 ^{o}C in the commercial base esters and 350 ^{o}C in the triglycerides, at which point a second C=O

stretching absorption characteristic of anhydrides develops at ~ 1846 cm^{-1}. The appearance of these bands implies that high concentrations of non-volatile radical species are present in the samples after C=C bond consumption is complete. The fact that radical recombination occurs at lower temperature in the commercial base ester samples than in the triglycerides implies a higher probability of radicals coming into close proximity with one another.[6] This is consistent with lower viscosity resulting from the resistance of the commercial base esters to oxidative polymerisation and crosslinking. Radical recombination products persist at temperatures above 500 ^{o}C in all esters except ester A and therefore have the potential to interfere with the adhesion of coatings applied to substrates heated to these temperatures.

Significant volatilisation and/or thermal degradation of oxidation products occurs from 250 ^{o}C onwards for all the samples except safflower oil and ester A, as evidenced by a large decrease in intensity across the entire spectral range. The disappearance of bands in the C-H stretching region indicates the thermal degradation/combustion of the high molecular weight products formed by crosslinking reactions, processes which are complete by 350 ^{o}C for esters A and B and coconut, sesame and castor oils, and 400 ^{o}C for safflower oil. The higher degradation completion temperature observed for safflower oil is related to its higher levels of alkyl chain unsaturation; safflower oil is capable of forming deposits with a greater degree of crosslinking and thus a higher thermal stability.

As observed for the poly-unsaturated methyl esters in section 3.1, a band at ~ 1612 cm^{-1} is evolved at 300 ^{o}C in all of the ester samples. The emergence of this band signifies the reaction between carbonyl species with the aluminium pan surface to form soap-like metal carboxylate complexes (scheme 3.4). These complexes persist at temperatures greater than 500 ^{o}C in all of the samples except ester A. They therefore give rise to the high levels of residue observed for the triglyceride samples by TGA and are potentially responsible for the occurrence of uncoated defects in hot dip metallic coatings. The chemical changes observed by ATR during the thermo-oxidative decomposition of the ester samples verify findings made by TGA and PDSC.

3.2.3.7 Residue Impact on 55Al-43Zn-2Si Coating Quality

The effect of triglyceride and commercial base ester unsaturation levels on 55Al-43Zn-2Si hot-dip coating quality was assessed by performing industrial hot dipping trials using representative triglycerides and commercial base esters (castor, sesame and cottonseed oils and esters A and B). Figure 3.21 shows images of areas containing uncoated defects in the castor oil, ester B and sesame oil metal-coated samples and a defect-free area in the ester A-treated sample.

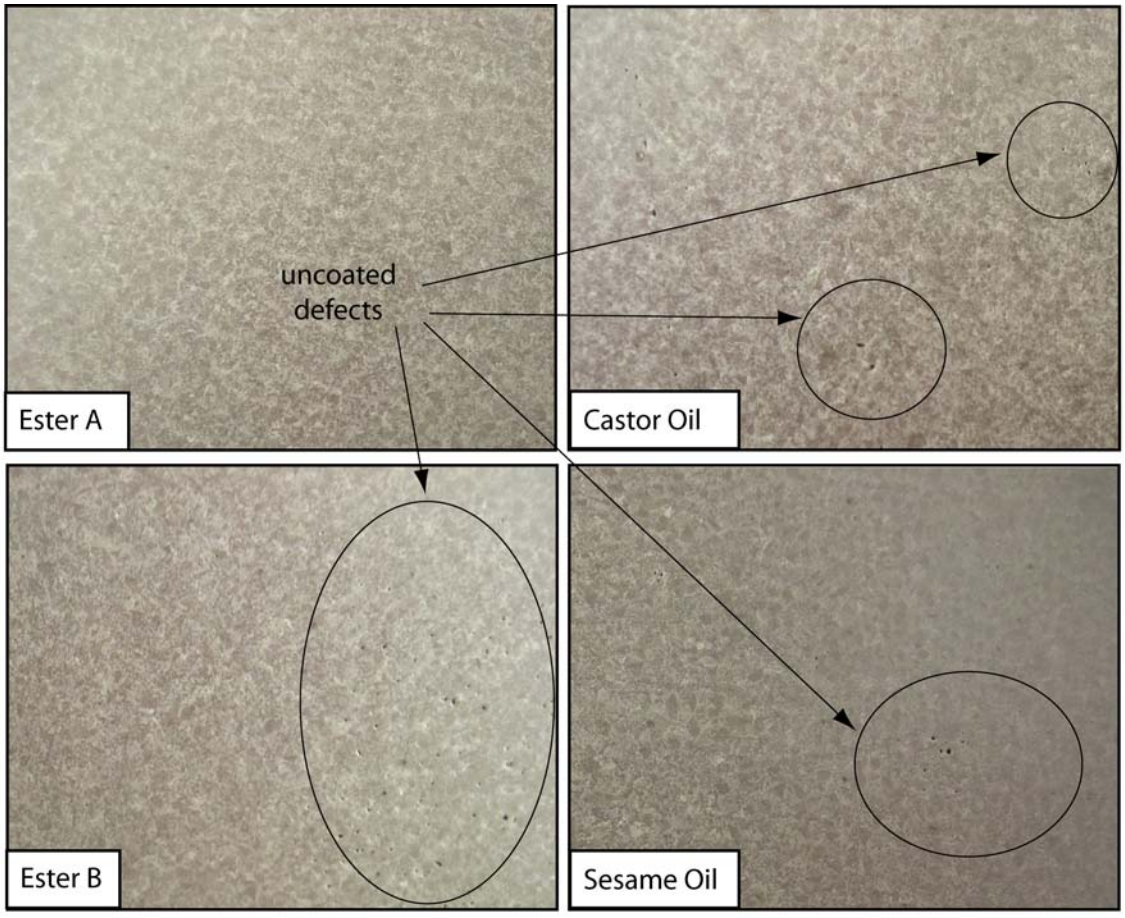

Figure 3.21 Photographs of 55Al-43.4Zn-1.6Si-coated industrial trial samples created using ester A, ester B, castor and sesame oil. Areas containing uncoated defects are highlighted.

SEM and optical microscopy images of one of these areas in the ester B sample are shown in figures 3.22A and 3.22B respectively.

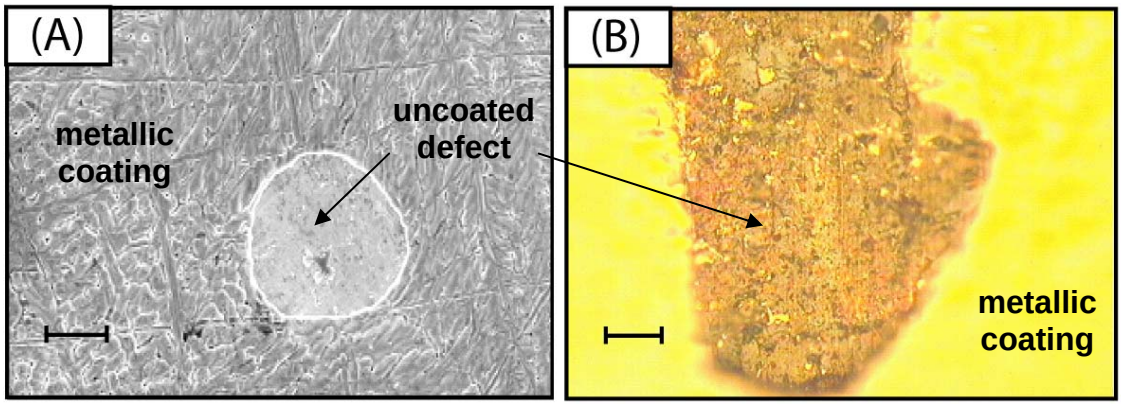

Figure 3.22 SEM micrograph (A, scale bar = 40μm) and an optical microscopy image (B, scale bar = 20μm) of uncoated defects in an ester B-treated industrial trial sample.

Figure 3.22 shows that the small, dark grey areas observed in the metal coated samples are uncoated defects. In figure 3.22B, a clear contrast between the alloy overlayer and the exposed steel substrate is apparent. The distance between the alloy overlayer surface and the steel substrate (the defect depth) is approximately 20 μm, equivalent to the average 55Al-43.4Zn-1.6Si coating thickness.[53] Similarly, the uncoated defect in the SEM micrograph appears as an oval-shaped blemish in the Zn-Al microstructure. X-ray analysis of the coated region surrounding the defect shows the presence of zinc and aluminium absorptions (figure 3.23). The absence of these absorptions in X-ray spectra acquired within the defect area and the presence of iron and oxygen absorptions confirms that the defect contains no alloy or intermetallic coating and is base-uncoated in nature, resulting from non-wetting of the steel surface by the molten alloy.[37, 38, 54-56]

The fact that the ester-treated samples produce coatings which contain more uncoated defects than a control sample (cold rolled steel with the original rolling oil film intact) is likely to be an artefact of the industrial trial method; removal of the original protective rolling oil film prior to ester application increases levels of substrate oxidation and could

result in increased levels of surface residue following the furnace cleaning process.[37, 54-58] Despite this, steel surface treatment with triglycerides or base esters of different alkyl chain unsaturation levels causes varied levels of uncoated defects.

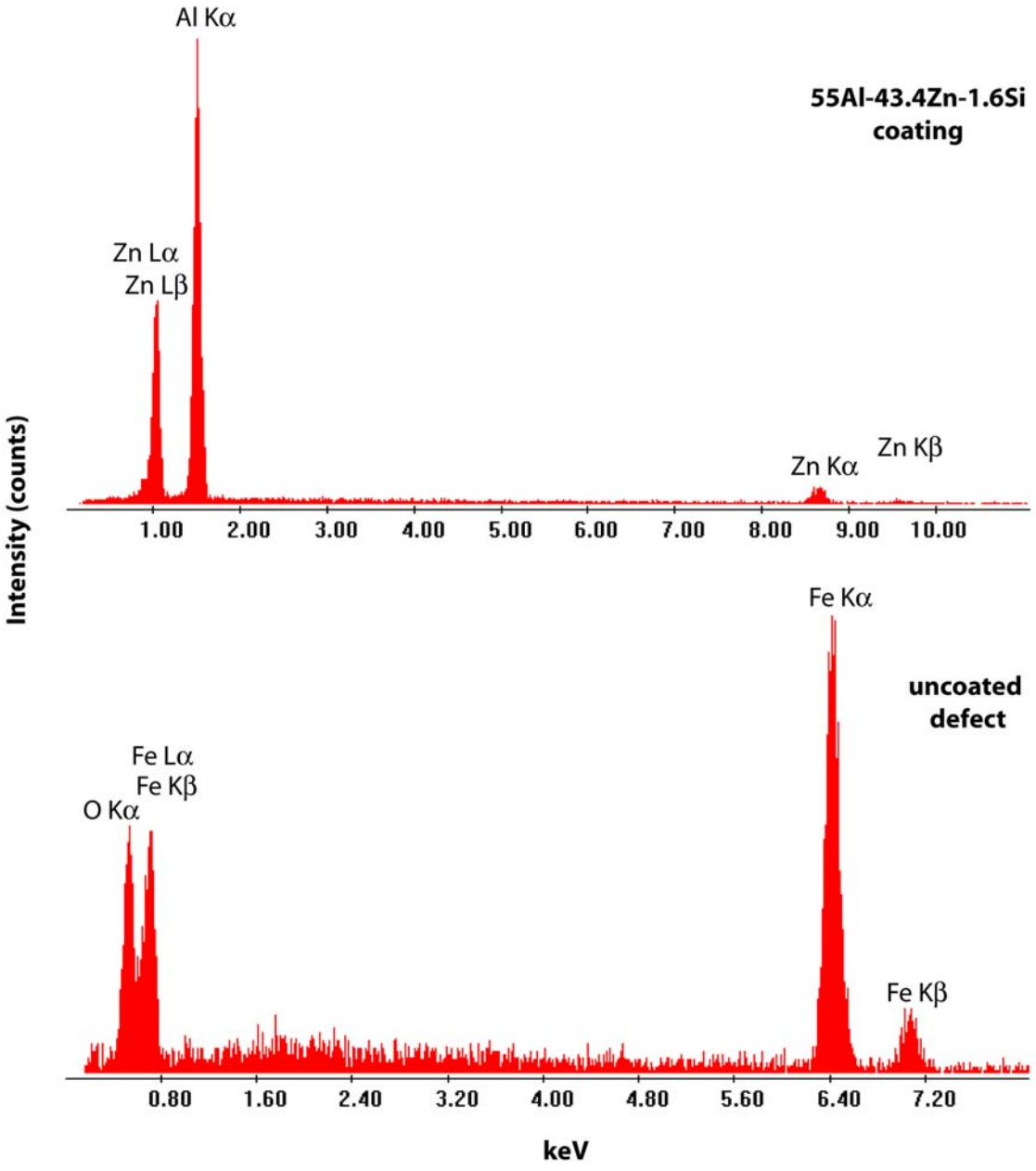

Figure 3.23 X-ray spectra acquired within a 55Al-43.4Zn-1.6Si coated area and an uncoated defect.

Cottonseed oil has comparatively little impact upon metallic coating quality; it contains very few uncoated defects and those that are present are distributed evenly and randomly across the surface and are tens to hundreds of microns (pinhole to fine uncoated), as opposed to millimetres (medium uncoated) or centimetres (gross uncoated), in dimension.[55] The sesame-oil treated sample is of marginally poorer quality with greater numbers of uncoated defects clustered together at several locations across the surface. Furthermore, the defects are larger in dimension (up to ~ 1 mm in diameter) than those observed in the cottonseed oil-treated sample. Finally, castor oil produces the poorest coating quality of the three triglycerides studied. Its uncoated defects are grouped together in clusters of ~ 50 or more at several locations across the sample surface and some areas contain defects that are ≥ 0.5 mm in size (fine to medium uncoated).

Analogous observations are made with respect to the commercial base ester samples; the ester B-treated sample contains significantly more uncoated defects than the sample prepared using ester A. In fact, more uncoated defects are present in the ester B-treated sample than in the castor oil sample and the defects are more severe in character, distributed over large regions of the sample surface and ranging from pinhole through to gross uncoated. These observations show that uncoated defect severity is directly related the ester alkyl chain unsaturation levels with cottonseed oil, the most saturated triglyceride (72 % w/w unsaturated alkyl chains), producing a coating which contains fewer uncoated defects than more highly unsaturated triglycerides such as sesame oil (85 % w/w unsaturated alkyl chains) and castor oil (96 % unsaturated alkyl chains). The size of the uncoated defects also increases with increasing ester unsaturation levels.

The metallic coating quality results are consistent with the findings made by TGA, PDSC and FTIR; ester alkyl chain unsaturation levels have an effect on the amount of thermally stable carboxylate and non-volatile oxygenated radical recombination product residues remaining following the ester thermo-oxidative decomposition process. The detection of uncoated defects infers and these residues interfere with the wettability of the steel surface by the molten alloy.[37, 38, 54-56]

Despite the occurrence of uncoated defects in the ester-treated samples, no variation in

spangle size is apparent. This is in good agreement with the findings of Willem et al.,[38] who found that steel surface pre-treatment in an oxidising furnace at temperatures of 450 ^{o}C or more was sufficient to lower levels of iron carboxylate surface residues and prevent mini-spangle defects. However, the ATR results shown above confirm the presence of carboxylate-type residues and the hot dip metallic coating results indicate that these residues interfere with metallic coating quality. The two sets of findings can be reconciled if the levels of carboxylate residue in the present study are low enough to preclude the formation of mini-spangles but still cause uncoated defects.

To semi-quantitatively gauge ester impact upon metallic coating quality, commercial base esters A, B and C and coconut oil were analysed using the experimental hot dipping method. Optical microscopy images of the coating results obtained for coconut oil and ester A, shown in figure 3.24, are representative of those obtained for the other esters.

As for the industrial trial samples, no detrimental impact upon spangle size is observed for any of the ester samples. In comparison to the steel control, ester A has no negative impact upon metallic coating quality; very few uncoated defects are apparent and those that are present are pinhole uncoated in nature.

In contrast, the coconut oil-treated sample displays several areas containing base uncoated defects (the dark grey regions highlighted in figure 3.24). These defects result from complete non-wetting of the steel surface by the molten alloy and appear as sections of exposed steel substrate containing no intermetallic or alloy overlayer coating.[37, 54, 55] Unlike ester A, the defects in the coconut oil sample are more severe and range from pinhole through to medium uncoated in dimension.

Figure 3.25 shows the % uncoated defect area determined for each of the ester samples. Esters A and C do not increase the % uncoated defect area outside the experimental error limits and produce coatings of similar quality to the steel control sample (% uncoated defect area = 1.2 % and 0.6 % respectively). In contrast, ester B and coconut oil increase the level of uncoated defects to 1.6 % and 2.1 % respectively. These results verify the industrial trial coating observations as ester B has a more severe detrimental impact upon metallic coating quality than ester A. They are also in accordance with %

B/A ratio, % residue and FTIR results described in the preceding sections. Esters A and C produce % B/A ratios by PDSC (1.6 % and 2.1 % respectively) and TGA (18 % and 8 % respectively) that are significantly lower than that of ester B (PDSC = 4.2 %; TGA = 34 %) and decompose to leave ~ 0 % residue at 500 ^{o}C, whilst ester B decomposes to leave ~ 3 %. Similarly, ester A decomposes to leave no detectable radical recombination product/carboxylate residues at 500 ^{o}C, in contrast to ester B. The % uncoated defect area results therefore verify that esters which decompose to form large amounts of radical recombination product/carboxylate residue impact detrimentally upon metallic coating quality.

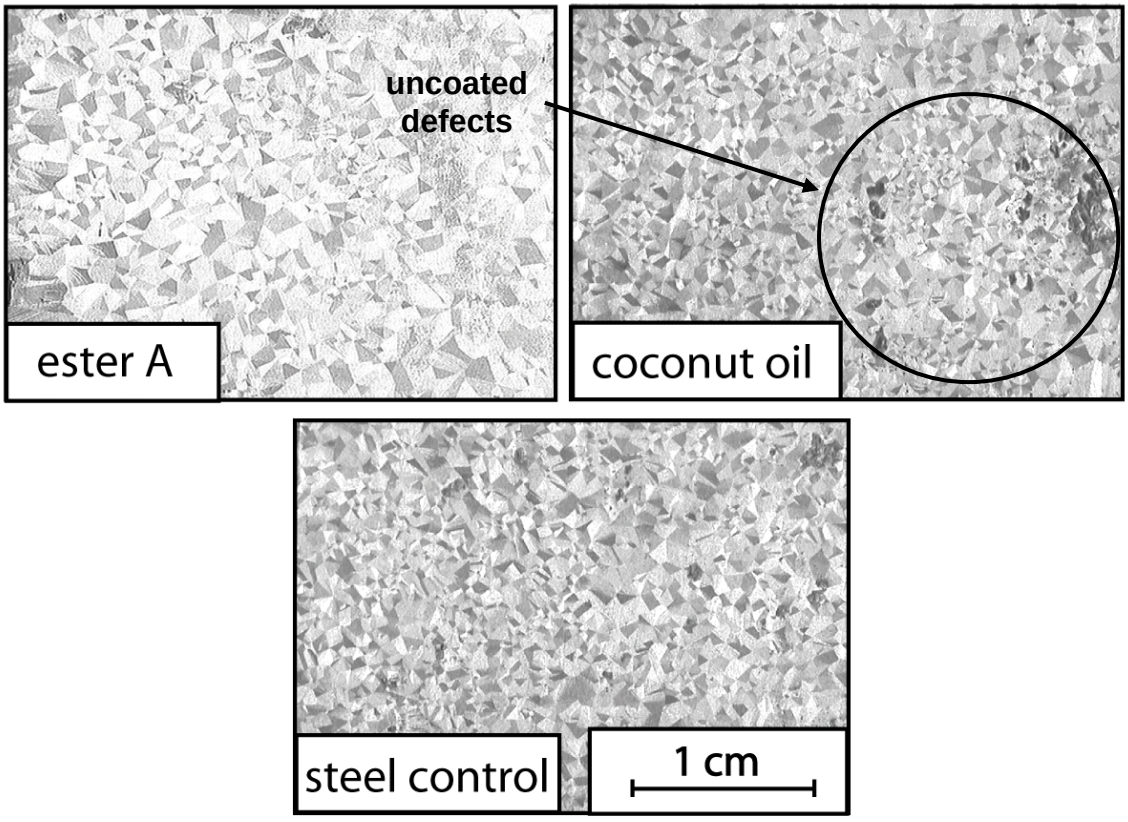

Figure 3.24 Optical microscopy images of 55Al-43.4Zn-1.6Si coated steel samples prepared using the hot dipping simulator after the application of ester A and coconut oil. A control sample prepared from untreated steel is shown for comparison.

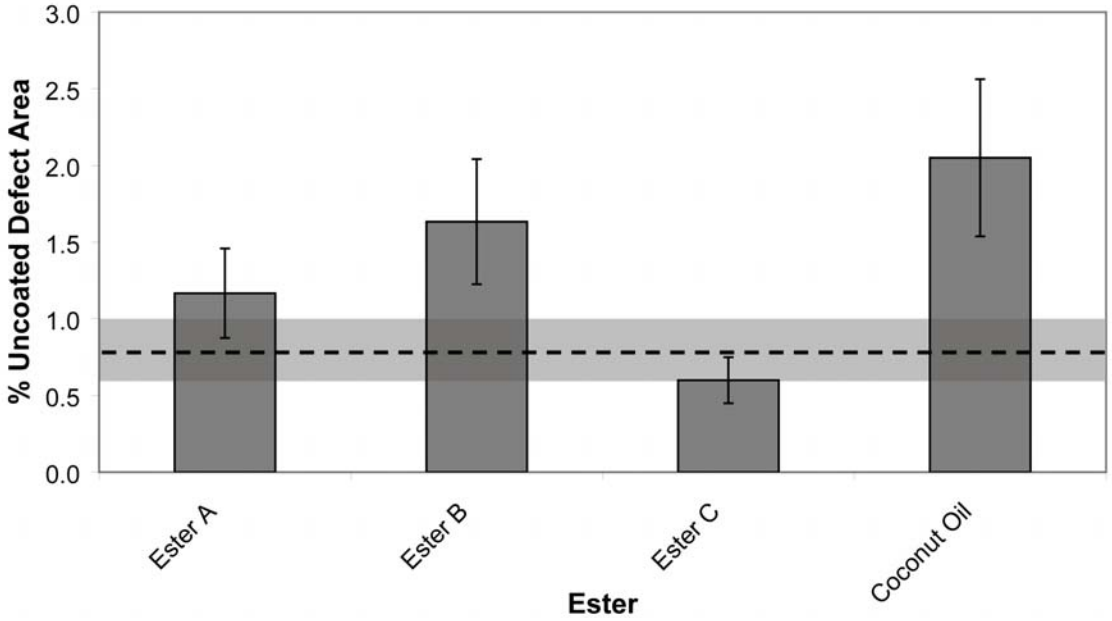

Figure 3.25 % uncoated defect area results for 55Al-43.4Zn-1.6Si coated samples prepared from steel treated with neat base esters A, B, C and coconut oil. The error bars represent ± 25 % error. The dashed line indicates the % uncoated defect area of the steel control (% uncoated defect area = 0.8 %) and the grey region indicates the associated error.

3.2.4 Conclusions

The thermo-oxidative and thermo-reductive decomposition properties of seven common triglycerides and three commercial cold rolling base esters have been studied by TGA and PDSC techniques. The results reveal that triglyceride alkyl chain chemical structure has a significant impact upon the process of thermo-decomposition with highly unsaturated triglycerides and castor oil (which contains an hydroxyl functionality in its alkyl chain structure) undergoing increased levels of mass loss/heat flow at high temperatures. Such triglycerides leave up to 46 % more thermo-oxidative decomposition residue at 500 ^{o}C than their more saturated counterparts, which is confirmed using the % B/A ratio technique.[7, 8]

Semi- and fully-synthetic base esters volatilise more effectively at lower temperatures than comparable triglycerides to leave a lesser amount of residue at 500 ^{o}C. Analysis of

several hydrogenated ester derivatives confirms the identity of mass loss/heat flow events associated with the presence of C=C bonds and that increased residue levels are associated with alkyl chain unsaturation levels. Infrared spectroscopic analysis of products formed during the thermo-oxidative decomposition process indicates that the residue formed by the triglycerides and semi-/fully-synthetic base esters comprises of carboxylate complexes and non-volatile radical recombination products.

Molecular weight is the dominant factor controlling volatilisation under an thermo-reductive HNX atmosphere and the levels of residue formed by some triglycerides are lowered by more than 75 % due to the preclusion of oxidation reactions such as crosslinking and the promotion of low-temperature volatilisation.

The results of industrial hot dipping trials and experimental hot dipping simulations show that the residues formed by the ester thermal decomposition process adversely interfere with hot dip metallic coating quality by cause the formation of uncoated defects. Increasing ester alkyl chain unsaturation levels exacerbate this effect by increasing both the size and number of uncoated defects formed.

3.3 References

1. Hasenhuettl, G. L., Fats and Fatty Oils. In *Kirk-Othmer Encyclopedia of Chemical Technology*, Kroschwitz, J. I., 'Ed."; John Wiley & Sons: New York, 2005; pp 801.

2. Coni, E., Podesta, E., Catone, T., *Thermochim. Acta* **2004,** *418*, 11.

3. Sathivel, S., Prinyawiwatkul, W., Negulescu, I., King, J., Basnayake, B., *J. Am. Oil Chem. Soc.* **2003,** *80*, 1131.

4. Dweck, J., Sampaio, C. M. S., *J. Therm. Anal. Cal.* **2004,** *75*, 385.

5. Santos, J. C. O., Santos, I. M. G., Conceicao, M. M., Porto, S. L., Trindade, M. F. S., Souza, A. G., Prasad, S., Fernandes, V. J., Araujo, A. S., *J. Therm. Anal. Cal.* **2004,** *75*, 419.

6. Oyman, Z. O., Ming, W., van der Linde, R., *Prog. Org. Coat.* **2005,** *54*, 198.

7. Zhang, Y., Perez, J. M., Pei, P., Hsu, S. M., *Lubr. Eng.* **1992,** *48*, 221.

8. Zhang, Y., Pei, P., Perez, J. M., Hsu, S. M., *Lubr. Eng.* **1992,** *48*, 189.

9. Santos, J. C. O., Santos, I. M. G., Souza, A. G., Sobrinho, E. V., Fernandes Jr., V. J., Silva, A. J. N., *Fuel* **2004,** *83*, 2393.

10. Gamlin, C. D., Dutta, N. K., Choudhury, N. R., Kehoe, D., Matisons, J., *Thermochim. Acta* **2002,** *392-393*, 357.

11. Senthivel, P., Joseph, M., Nagar, S. C., Anoop, K., Naithani, K. P., Mehta, A. K., Raje, N. R., *NLGI Spokesman* **2005,** *69*, 26.

12. Kauffman, R. E., Rhine, W. E., *Lubr. Eng.* **1988,** *44*, 154.

13. Sharma, B. K., Stipanovic, A. J., *Thermochim. Acta* **2003,** *402*, 1.

14. Keyser, A. G., Kunkel, K. F., Snedaker, L. A., *Iron Steel Eng.* **1998,** *75*, 43.

15. Osten-Sacken, J., Pompe, R., Skold, R., *Thermochim. Acta* **1985,** *95*, 431.

16. Shen, L., Alexander, K. S., *Thermochim. Acta* **1999,** *340-341*, 271.

17. Porter, N. A., Mills, K. A., Carter, R. L., *J. Am. Chem. Soc.* **1994,** *116*, 6690.

18. Frankel, E. N., *Prog. Lipid Res.* **1985,** *23*, 197.

19. Cheenkachorn, K., Lloyd, W. A., Perez, J. M. In *The use of pressurized differential scanning calorimetry (PDSC) to evaluate effectiveness of additives in vegetable oil lubricants*, ASME ICES03, Spring Technical Conference, Internal Combustion Engine Division, Saltzburg; May 11-15, 2003, pp 197.

20. Adhvaryu, A., Erhan, S. Z., Liu, Z. S., Perez, J. M., *Thermochim. Acta* **2000,** *364*, 87.

21. Dunn, R., *Trans. ASABE* **2006,** *49*, 1633.

22. Abou El Naga, H. H., Salem, A. E. M., *Wear* **1984,** *96*, 267.

23. Suilen, F., Zuurbier, S. In *Fundamental aspects of gas-metal reactions during batch annealing in 100% hydrogen*, Proc. 38th Mechanical Working and Steel Processing Conference, Ohio, USA; 1997, pp 375.

24. Gines, M. L. J., Benitez, G. J.,Perez, T., Bossi, E. In *Surface reactions during batch annealing process*, Proc. 55th Annual ABM Congress, Rio de Janeiro; 2000, pp 2239.

25. Gracia-Fernandez, C. A., Gomez-Barriero, S., Ruiz-Salvador, S., Blaine, R., *Prog. Org. Coat.* **2005,** *54*, 332.

26. Bana De Schor, B., Toni, J. E., *Thermochim. Acta* **1976,** *16*, 365.

27. Williams, D. H., Fleming, I., *Spectroscopic Methods in Organic Chemistry*. 5 ed.; McGraw-Hill Publishing Company: England, 1997.

28. Vogel, A. I., Tatchell, A. R., Furnis, B. S., Hannaford, A. J., Smith, P. W. G., *Vogel's Textbook of Practical Organic Chemistry, 5th edition*. Addison Wesley Longman Ltd: London, UK, 1989.

29. Hanaki, K., *Sumimoto Light M. Tech.* **1984,** *25*, 44.

30. Svedung, D. H., *Scand. J. Metall.* **1980,** *9*, 183.

31. De Werbier, P., Hocquaux, H., Flandin-Rey, Y., Jacquet, D., *Development of new methods of analysis for organic compounds on the surface of steel products*; EUR 14113; Luxembourg, 14-16 May 1991, 1992; pp 101.

32. Shamaiengar, M., *Iron Steel Eng.* **1967,** *44*, 135.

33. Sech, J. M., Oleksiak, T. P., *Iron Steel Eng.* **1995,** *72*, 33.

34. Chopra, A., Sastry, M. I. S., Kapur, G. S., Sarpal, A. S., Jain, S. K., Srivastava, S. P., Bhatnagar, A. K., *Lubr. Eng.* **1995,** *52*, 279.

35. Fox, N. J., Stachowiak, G. W., *Lubr. Eng.* **2003,** *59*, 15.

36. Treverton, J. A., Thomas, M. P., *Int. J. Adhes. Adhes.* **1989,** *9*, 211.

37. Tang, N.-Y., Goodwin, F. E. In *A study of defects in galvanized coatings*, Galvatech '01 - Proc. 5th Int. Conf. on Zinc and Zinc Alloy Coated Steel Sheet, Brussels, Belgium; 2001, pp 49.

38. Willem, J.-F., Claessens, S., Cornil, H., Fiorucci, M., Hennion, A., Xhoffer, C. In *Solidification mechanisms of aluzinc coatings - effect on spangle size*, Galvatech '01 - Proc. 5th Int. Conf. on Zinc and Zinc Alloy Coated Steel Sheet, Brussels, Belgium; 2001, pp 401.

39. Pilon, A. C., Cole, K. C., Noel, D. In *Surface characterization of cold-rolled steel by grazing-angle reflection-absorption FT-IR spectroscopy*, SPIE Proc. - 7th Int. Conf. on Fourier Transform Spectrosc., 1989, pp 209.

40. Tusset, V., Muller, V., *Chemical analysis of oils present on steel sheet*; EUR 14113; 1992; pp 108.

41. Hombek, R., Heenan, D. F., Januszkiewicz, K. R., Sulek, H. H., *Lubr. Eng.* **1989,** *45*, 56.

42. Zeman, A., Stuwe, R., Koch, K., *Thermochim. Acta* **1984,** *80*, 1.

43. Tamai, Y., Sumimoto, M., *Lubr. Eng.* **1975,** *31*, 81.

44. Kowalski, B., *Thermochim. Acta* **1993,** *213*, 135.

45. Kodali, D. R., *J. Agric. Food Chem.* **2005,** *53*, 7649.

46. Kasprzycka-Guttman, T., Odzeniak, D., *J. Therm. Anal.* **1993,** *39*, 217.

47. Vora, A., Riga, A. Dollimore, D., Alexander, K. S., *Thermochim. Acta* **2002,** *392-393*, 209.

48. Rice, F. O., Herzfeld, K. F., *J. Am. Chem. Soc.* **1934,** *56*, 284.

49. Adhvaryu, A., Erhan, S. Z., Sahoo, S. K., Singh, I. D., *Fuel* **2002,** *81*, 785.

50. Du, D., Kim, S. -S., Moon, W. -S., Jin, S. -B., Kwon, W. -S., *Thermochim. Acta* **2003,** *407*, 17.

51. Knothe, G., *Fuel Process.Technol.* **2005,** *86*, 1059.

52. Saito, T., Hayamizu, K., Yanagisawa, M., Yamamoto, O. Spectral Database for Organic Compounds, SDBS. http://riodb01.ibase.aist.go.jp/sdbs/cgi-bin/cre_index.cgi?lang=eng (22/07/07).

53. Townsend, H. E., Continuous Hot Dip Coatings. In *ASM Handbook - Surface Engineering*; ASM International (The Materials Information Society): 1994; 'Vol.' 5, pp 339.

54. Chen, F., Patil, R. In *An in-depth analysis of various subtle coating defects of the 2000's*, Galvatech '04 - Proc. 6th Int. Conf. on Zinc and Zinc Alloy Coated Steel Sheet, Chicago, USA; 2004, pp 1055.

55. Browne, K. M., *Zincalume pinhole uncoated investigation: progress report*; 726; John Lysaght (Australia) Limited: April, 1980; pp 1.

56. Puente, J. M., Alonso, F. J., Andres, L., Prado, M. In *Influence of an adequate surface conditioning on the final characteristics of GI for exposed panels use on automotive sector*, Galvatech '04 - Proc. 6th Int. Conf. on Zinc and Zinc Alloy Coated Steel Sheet, Chicago, USA; 2004, pp 457.

57. Durandet, Y., Ebrill, N., Strezov, L. In *Influence of substrate oxidation on dynamic wetting, interfacial resistance and surface appearance of Al-Zn-Si hot dip coatings*, Proc. PacZAC '99, Kuala Lumpur, Malaysia; 1999.
58. Ebrill, N., Durandet, Y., Strezov, L. In *Influence of substrate oxidation on dynamic wetting, interfacial resistance and surface appearance of hot dip coatings*, Galvatech '01 - Proc. 5th Int. Conf. on Zinc and Zinc Alloy Coated Steel Sheet, Brussels, Belgium; 2001, pp 351.